

UNITED STATES
DEPARTMENT OF
COMMERCE
PUBLICATION



NBS TECHNICAL NOTE 717

Methods of Measurement for Semiconductor Materials, Process Control, and Devices

U.S.
DEPARTMENT
OF
COMMERCE

National
Bureau
of
Standards

5753
0.717
972

Quarterly Report
July 1 to September 30, 1971

NATIONAL BUREAU OF STANDARDS

The National Bureau of Standards¹ was established by an act of Congress March 3, 1901. The Bureau's overall goal is to strengthen and advance the Nation's science and technology and facilitate their effective application for public benefit. To this end, the Bureau conducts research and provides: (1) a basis for the Nation's physical measurement system, (2) scientific and technological services for industry and government, (3) a technical basis for equity in trade, and (4) technical services to promote public safety. The Bureau consists of the Institute for Basic Standards, the Institute for Materials Research, the Institute for Applied Technology, the Center for Computer Sciences and Technology, and the Office for Information Programs.

THE INSTITUTE FOR BASIC STANDARDS provides the central basis within the United States of a complete and consistent system of physical measurement; coordinates that system with measurement systems of other nations; and furnishes essential services leading to accurate and uniform physical measurements throughout the Nation's scientific community, industry, and commerce. The Institute consists of a Center for Radiation Research, an Office of Measurement Services and the following divisions:

Applied Mathematics—Electricity—Heat—Mechanics—Optical Physics—Linac Radiation²—Nuclear Radiation²—Applied Radiation²—Quantum Electronics³—Electromagnetics³—Time and Frequency³—Laboratory Astrophysics³—Cryogenics³.

THE INSTITUTE FOR MATERIALS RESEARCH conducts materials research leading to improved methods of measurement, standards, and data on the properties of well-characterized materials needed by industry, commerce, educational institutions, and Government; provides advisory and research services to other Government agencies; and develops, produces, and distributes standard reference materials. The Institute consists of the Office of Standard Reference Materials and the following divisions:

Analytical Chemistry—Polymers—Metallurgy—Inorganic Materials—Reactor Radiation—Physical Chemistry.

THE INSTITUTE FOR APPLIED TECHNOLOGY provides technical services to promote the use of available technology and to facilitate technological innovation in industry and Government; cooperates with public and private organizations leading to the development of technological standards (including mandatory safety standards), codes and methods of test; and provides technical advice and services to Government agencies upon request. The Institute also monitors NBS engineering standards activities and provides liaison between NBS and national and international engineering standards bodies. The Institute consists of the following divisions and offices:

Engineering Standards Services—Weights and Measures—Invention and Innovation—Product Evaluation Technology—Building Research—Electronic Technology—Technical Analysis—Measurement Engineering—Office of Fire Programs.

THE CENTER FOR COMPUTER SCIENCES AND TECHNOLOGY conducts research and provides technical services designed to aid Government agencies in improving cost effectiveness in the conduct of their programs through the selection, acquisition, and effective utilization of automatic data processing equipment; and serves as the principal focus within the executive branch for the development of Federal standards for automatic data processing equipment, techniques, and computer languages. The Center consists of the following offices and divisions:

Information Processing Standards—Computer Information—Computer Services—Systems Development—Information Processing Technology.

THE OFFICE FOR INFORMATION PROGRAMS promotes optimum dissemination and accessibility of scientific information generated within NBS and other agencies of the Federal Government; promotes the development of the National Standard Reference Data System and a system of information analysis centers dealing with the broader aspects of the National Measurement System; provides appropriate services to ensure that the NBS staff has optimum accessibility to the scientific information of the world, and directs the public information activities of the Bureau. The Office consists of the following organizational units:

Office of Standard Reference Data—Office of Technical Information and Publications—Library—Office of International Relations.

¹ Headquarters and Laboratories at Gaithersburg, Maryland, unless otherwise noted; mailing address Washington, D.C. 20234.

² Part of the Center for Radiation Research.

³ Located at Boulder, Colorado 80302.

16 1972

stace

RC 100

05753

no. 717

1972

Methods of Measurement for Semiconductor Materials, Process Control, and Devices

Quarterly Report, July 1 to September 30, 1971

W. Murray Bullis, Editor

Electronic Technology Division
Institute for Applied Technology
National Bureau of Standards
Washington, D.C. 20234

Jointly Supported by:

The National Bureau of Standards,
The Defense Nuclear Agency,
The U.S. Navy Strategic Systems Project Office,
The U.S. Navy Electronic Systems Command,
The Air Force Weapons Laboratory,
The Air Force Cambridge Research Laboratories,
The Advanced Research Projects Agency,
The Atomic Energy Commission, and
The National Aeronautics and Space Administration.



U.S. DEPARTMENT OF COMMERCE, Peter G. Peterson, Secretary
U.S. NATIONAL BUREAU OF STANDARDS, Lewis M. Branscomb, Director,

Issued April 1972

Technical note no. 717.

National Bureau of Standards Technical Note 717

Nat. Bur. Stand. (U.S.), Tech. Note 717, 52 pages (Apr. 1972)

CODEN: NBTNAE

Issued April 1972

For sale by the Superintendent of Documents, U.S. Government Printing Office
Washington, D.C. 20402 (Order by SD Catalog No. C 13.46:717). Price 55 cents.

CONTENTS

	PAGE
Foreword	vi
1. Introduction	1
2. Highlights	3
3. Methods of Measurement for Semiconductor Materials	
3.1. Resistivity	6
3.2. Gold-Doped Silicon	10
3.3. Infrared Methods	13
3.4. Specification of Germanium	17
3.5. References	18
4. Methods of Measurement for Process Control	
4.1. Die Attachment Evaluation	19
4.2. Wire Bond Evaluation	22
4.3. References	30
5. Methods of Measurement for Semiconductor Devices	
5.1. Thermal Properties of Devices	31
5.2. Thermographic Measurements	32
5.3. Microwave Device Measurements	34
5.4. Carrier Transport in Junction Devices	36
5.5. Silicon Nuclear Radiation Detectors	40
5.6. References	42
Appendix A. Joint Program Staff	43
Appendix B. Committee Activities	44
Appendix C. Solid-State Technology & Fabrication Services	46
Appendix D. Joint Program Publications	47

LIST OF FIGURES

	PAGE
1. Typical reverse current-voltage characteristic for a 0.5-mm diameter silicon diode prepared for capacitance-voltage measurements	8
2. Resistivity as a function of gold concentration in initially <i>n</i> -type silicon	11
3. Infrared response spectra of two lithium-drifted, germanium gamma-ray detectors	14
4. Comparison of the digital form of an infrared response spectrum as displayed on the oscilloscope of a multi-channel analyzer system with a directly obtained strip chart recording of the same spectrum	15
5. Infrared response spectrum of a lithium-drifted, silicon detector after neutron irradiation	16
6. Percent increase in average junction-to-case temperature difference of diodes with voids over that of their respective controls measured under steady-state and transient conditions as a function of percent void area in the diode die attachment	21
7. Schematic representation of device structure assumed in calculation of wire-bond flexure	23
8. Wire-bond flexure as a function of power dissipation for triangular and semicircular loops with several values of initial height	25
9. SEM photomicrograph of a rectangular wire-feed hole in an ultrasonic bonding tool	26
10. Most desirable placement position for capacitor microphone used in study of variations in vibration amplitudes of the bonding tool at the fundamental driving frequency and its harmonics during bonding	27
11. A relatively stable waveshape observed 5 to 10 ms after the start of bonding showing individual differences in the harmonic content from peak to peak	28
12. Measured pull strength as a function of bond angle (θ)	29

13.	Common-base circuit for measuring thermal resistance of transistors using the collector-base voltage as the temperature sensitive parameter	32
14.	Equivalent circuit used to model a transistor for analysis of delay-time measurements	38

LIST OF TABLES

1.	Transitions in Neutron-Irradiated, Lithium-Drifted Silicon Detector	17
2.	Summary of Results of Junction-to-Case Temperature Difference Measurements	20

FOREWORD

The Joint Program on Methods of Measurement for Semiconductor Materials, Process Control, and Devices was undertaken in 1968 to focus NBS efforts to enhance the performance, interchangeability, and reliability of discrete semiconductor devices and integrated circuits through improvements in methods of measurement for use in specifying materials and devices and in control of device fabrication processes. These improvements are intended to lead to a set of measurement methods which have been carefully evaluated for technical adequacy, which are acceptable to both users and suppliers, which can provide a common basis for the purchase specifications of government agencies, and which will lead to greater economy in government procurement. In addition, such methods will provide a basis for controlled improvements in essential device characteristics, such as uniformity of response to radiation effects.

The Program is supported by the National Bureau of Standards,* the Defense Atomic Support Agency,[†] the U.S. Navy Strategic Systems Project Office,[§] the U.S. Navy Electronics Systems Command,[†] the Air Force Weapons Laboratory,[¶] the Air Force Cambridge Research Laboratories,[#] the Advanced Research Projects Agency,[×] the Atomic Energy Commission,** and the National Aeronautics and Space Administration.^{††} Although there is not a one-to-one correspondence between the tasks described in this report and the cost centers through which the Program is supported, the concern of certain sponsors with specific parts of the program is reflected in planning and conduct of the work.

* Through Research and Technical Services Cost Centers 4251126, 4252128, and 4254115.

† Through Order EA071-801. (NBS Cost Center 4259522).

§ Administered by U.S. Naval Ammunition Depot, Crane, Indiana through Project Order PO-2-0023. (NBS Cost Center 4259533).

† Through Project Order PO-2-1034. (NBS Cost Center 4252534).

¶ Through Delivery Order F29601-71-F-0002. (NBS Cost Center 4252535).

Through Project Order Y71-906. (NBS Cost Center 4251536).

× ARPA Order 1889 Monitored by Space and Missile Systems Organization under MIPR FY76167100331. (NBS Cost Center 4254422).

** Division of Biology and Medicine. (NBS Cost Center 4259425).

†† Through Order S-70003-G, Goddard Space Flight Center. (NBS Cost Center 4254429).

METHODS OF MEASUREMENT FOR SEMICONDUCTOR MATERIALS, PROCESS CONTROL, AND DEVICES

Quarterly Report
July 1 to September 30, 1971

ABSTRACT

This quarterly progress report, thirteenth of a series, describes NBS activities directed toward the development of methods of measurement for semiconductor materials, process control, and devices. Significant accomplishments during this reporting period include the disclosure of substantial differences in measurements of transistor delay time, a device characteristic frequently used as a screen in radiation hardness assurance tests, as measured with two different instruments; successful application of the infrared response technique to the study of radiation-damaged, lithium-drifted silicon detectors; and identification of a condition that minimizes wire flexure and reduces the failure rate of wire bonds in transistors and integrated circuits under slow thermal cycling conditions. Work is continuing on measurement of resistivity of semiconductor crystals; study of gold-doped silicon; specification of germanium for gamma-ray detectors; evaluation of wire bonds and die attachment; measurement of thermal properties of semiconductor devices, delay time and related carrier transport properties in junction devices, and noise properties of microwave diodes; and characterization of silicon nuclear radiation detectors. Supplementary data concerning staff, standards committee activities, technical services, and publications are included as appendixes.

Key Words: Alpha-particle detectors; aluminum wire; base transit time; carrier lifetime; die attachment; electrical properties; epitaxial silicon; gamma-ray detectors; germanium; gold-doped silicon; infrared response; methods of measurement; microelectronics; microwave diodes; nuclear radiation detectors; probe techniques (a-c); resistivity; semiconductor devices; semiconductor materials; semiconductor process control; silicon; thermal resistance; thermographic measurements; ultrasonic bonding; wire bonds.

1. INTRODUCTION

This is the thirteenth quarterly report to the sponsors of the Joint Program on Methods of Measurement for Semiconductor Materials, Process Control, and Devices. It summarizes work on a wide variety of measurement

INTRODUCTION

methods that are being studied at the National Bureau of Standards. Since the Program is a continuing one, the results and conclusions reported here are subject to modification and refinement.

The work of the Program is divided into a number of tasks, each directed toward the study of a particular material or device property or measurement technique. This report is subdivided according to these tasks. Highlights of activity during the quarter are given in Section 2. Section 3 deals with tasks on methods of measurement for materials; Section 4, with those on methods of measurement for process control; and Section 5, with those on methods of measurement for devices. References for each section are listed in a separate subsection at the end of that section.

The report of each task includes the long-term objective, a narrative description of progress made during this reporting period, and a listing of plans for the immediate future. Additional information concerning the material reported may be obtained directly from individual staff members connected with the task as indicated throughout the report. The organization of the Joint Program staff and telephone numbers are listed in Appendix A.

An important part of the work that frequently goes beyond the task structure is participation in the activities of various technical standardizing committees. The list of personnel involved with this work given in Appendix B suggests the extent of this participation. Additional details of current efforts in this area are given in Section 2.

Background material on the Program and individual tasks may be found in earlier reports in this series as listed in Appendix D. From time to time, publications that describe some aspect of the program in greater detail are prepared. Current publications are also listed in Appendix D.

2. HIGHLIGHTS

Significant accomplishments during this reporting period include successful application of the infrared response technique to the study of radiation-damaged, lithium-drifted silicon detectors; identification of a condition that minimizes wire flexure and reduces the failure rate of transistors under slow-thermal cycling conditions; and completion of initial intercomparison measurements of transistor delay time made with two different circuits. Highlights of these and other technical activities are presented in this section; details are given in subsequent sections of the report. This section concludes with a summary of standardization activities being carried out by program staff members.

Resistivity — Measurements of the current and probe-force dependence of four-probe measurements on lapped specimens were completed. Compared with the mechanical and chem-mechanically polished surfaces of the same wafers previously measured, lapped surfaces exhibit resistivity values several tenths of a percent higher than chem-mechanically polished surfaces, and several tenths of a percent lower than mechanically polished surfaces. General current and pressure dependences are the same for all surfaces. A modification of the collaborative reference program is under consideration as an appropriate mechanism for providing resistivity standards to the industry. Attempts to locate the source of low yield of diodes used in the study of the capacitance-voltage method indicated that none of the steps in the mechanical processing of in-house diodes affected diode yield if they were followed by chem-mechanical polish prior to diffusion. Work on detailed study of the relationship between the four-probe and capacitance-voltage measures of resistivity continued.

Gold-Doped Silicon — Resistivity measurements on gold-doped *n*-type silicon wafers and diffusions of gold into *p*-type silicon wafers were made as scheduled and analyzed. Several short-time diffusions and annealing treatments were made to study effects due to interstitial gold and precipitation of gold, respectively. Additional preliminary measurements of carrier lifetime in gold-diffused wafers were made by the surface photovoltage method.

Infrared Methods — The infrared response (IRR) technique was used to study nine germanium diodes; the presence of lithium precipitate clusters was tentatively identified in two diodes. Initial IRR measurements on three lithium-drifted silicon detectors, two of which had been subjected to radiation damage, revealed features at energies associated with divacancies, vacancy-oxygen pairs, and lithium precipitates. A second cryostat has been constructed for use with this technique, and the system for converting the analog output of the IRR system into digital form was put into use.

Die Attachment Evaluation — Measurements of steady-state thermal response and transient thermal response for heating-power pulse widths

HIGHLIGHTS

ranging from 5 to 100 ms were made on several additional groups of diodes bonded to TO-5 headers with dimples ultrasonically machined into the bonding surface to provide voids of known size. The spread in thermal response of the group of devices with 20-percent void areas was significantly improved over the spread reported previously for devices which had the same 20-percent dimple area in the header in accord with the finding that some of the previously bonded devices had void areas larger than the dimple. For the various groups of devices the percent increase in sensitivity to voids of transient thermal response over the steady-state thermal response measurements varied from 123 percent to 333 percent. The increase in average steady-state thermal response of the devices with 10 percent void areas over that of their controls was of the same order as the sample standard deviation of the controls for these groups and therefore does not yield a useful indication of the presence of voids. A theoretical study was undertaken to ascertain the limitations of thermal response techniques for detecting poor die adhesion in the devices under investigation.

Wire Bond Evaluation — Additional calculations have been carried out to examine the problem of thermal-expansion-induced wire bond-loop flexing in more detail. Application of a minimum loop-height specification based on the results of these calculations to a production run of transistors has resulted in a dramatic decrease in failure due to slow thermal cycling. Progress was made in adapting ribbon-wire bonding techniques to a production environment. Work was resumed on the study of bonding tool motion during bonding by means of a capacitor microphone. This work is directed toward the eventual development of an in-process control technique for the evaluation of bonds. Work on evaluation of the destructive, double-bond, pull test has resumed with the continuation of experiments to test the effects on the measured pull strength of single-level bond pairs of variation in pull rate, pull angle, and hook position. Results of a second series of tests to determine the effect of variations in bond angle on the measured pull strength of single-level bond pairs pulled vertically at the center of the loop did not agree with the results obtained previously.

Thermal Properties of Devices — The common-base thermal resistance measuring circuit using the transistor emitter-base voltage as the temperature sensitive parameter, was modified so that the collector-base voltage could also be used as the temperature sensitive parameter to measure thermal resistance. A single test unit with as much common circuitry as possible was built to facilitate the comparison of these methods with the common-emitter, base-and-collector switching technique using the transistor base-emitter voltage as the temperature sensitive parameter.

Microwave Device Measurements — A group of 1N23 diodes was measured for insertion loss to obtain detailed reproducibility data on the waveguide system. The system was then modified by the introduction of new, rigid base plates and clamping-type supports. The rotary-vane attenuator

HIGHLIGHTS

was modified by the addition of two lockable vernier micrometer heads. Visits were made to two major suppliers of microwave mixer diodes in order to discuss measurement requirements for mixer diodes and to obtain information and guidance for the planning of future activities in the mixer diode area.

Carrier Transport in Junction Devices - Preliminary intercomparison measurements of transistor delay time have been made on the Sandia bridge and vector voltmeter. Under some conditions of measurement, significantly different values were obtained for this characteristic that is frequently used as a screen in radiation hardness assurance tests. Both S-parameter systems have been assembled and familiarization tests begun. Additional study has been completed on the problem of high frequency electrical probing of semiconductor devices at the wafer stage. An analysis was completed which relates delay time as measured by the Sandia bridge and the vector voltmeter to internal device time constants.

Standardization Activities - Many of the standardization activities undertaken by program staff are broader than the technical tasks described in the following sections. These activities involve general staff support in committees, coordination of efforts which may encompass a variety of tasks, and participation in areas where no direct in-house technical effort is underway. Standardization activities directly related to particular task areas are reported with the appropriate tasks.

Seven program staff members attended the regular fall meeting of ASTM Committee F-1 on Electronics, in Boston. The new section on Bonding continued to show considerable vitality with an attendance of nearly 30. Program staff members accepted responsibility for preparing a number of new and revised methods including measurement of carrier lifetime by the surface photovoltage method, measuring resistivity profiles by the spreading resistance method, and three leak detection methods. Two documents were edited at the committee level and four at the subcommittee level by program staff members.

Activity in connection with JEDEC committees of the Electronic Industries Association was hampered by the cancellation of several meetings of committees and task groups during the quarter.

Two program staff members attended meetings of SAE Subcommittee A-2N on Radiation Hardness and Nuclear Survivability and of ASTM Subcommittee E-10.07 on Radiation Effects on Electronic Materials held in July in connection with the IEEE Annual Conference on Nuclear and Space Radiation Effects.

3. METHODS OF MEASUREMENT FOR SEMICONDUCTOR MATERIALS

3.1. RESISTIVITY

Objective: To develop methods suitable for use throughout the electronics industry for measuring resistivity of bulk, epitaxial, and diffused silicon wafers.

Progress: Measurements of the current and probe-force dependence of four-probe measurements on lapped specimens were completed. Compared with the mechanical and chem-mechanically polished surfaces of the same wafers previously measured, lapped surfaces exhibit resistivity values several tenths of a percent higher than chem-mechanically polished surfaces, and several tenths of a percent lower than mechanically polished surfaces. General current and pressure dependences are the same for all surfaces. A modification of the collaborative reference program is under consideration as an appropriate mechanism for providing resistivity standards to the industry. Attempts to locate the source of low yield of diodes used in the study of the capacitance-voltage method indicated that none of the steps in the mechanical processing of in-house diodes affected diode yield if they were followed by a chem-mechanical polish prior to diffusion. Work on detailed study of the relationship between the four-probe and capacitance-voltage measures of resistivity continued.

Four-Probe Method - Measurement of the current and probe-force dependence of resistivity by the four-probe method continued. Measurements were made on lapped surfaces of the same wafers used previously with other surface conditions. Each wafer exhibited the same general dependence on current and probe force that had been observed on mechanically and chem-mechanically polished surfaces of the same specimens. In all cases wafer surfaces mechanically polished with 0.3 μm diamond grit yield the highest measured resistivity values. Lapped surfaces yield values a few tenths to perhaps 1 percent lower, and chem-mechanically polished surfaces yield values a few tenths of a percent lower still. In most cases the sample standard deviation associated with measurements made under a given set of conditions was of the order of 0.5 percent or less. It has been found that the apparent current dependence of some wafers was due to order of current sampling as well as to current level but the two effects have not yet been separated.

These results and those obtained from measurements made on lapped surfaces at the beginning of this experiment cannot be compared satisfactorily. Although the precision of measurements made under the same current and probe-force conditions shows very little variation between the two sets of data, considerably greater variation of the measured average resistivity value on current and probe force was found in the earlier data. These large variations in the earlier data were erratic functions of current and probe force and apparently resulted in part from inadequate

RESISTIVITY

control of unsuspected variables in the experiment. The tighter experimental control initiated after the original set of data was completed is probably responsible for the reduction of this erratic variability in the present results. (D. R. Ricks and J. R. Ehrstein)

No further work has been done on the study of subsurface damage in silicon slices as a result of various steps of wafer preparation. Previous work using an infrared photovoltage technique pointed out the need for a infrared detector with better sensitivity than that being used. An improved detector has been installed and the system is again operational. (W. R. Thurber and W. E. Phillips)

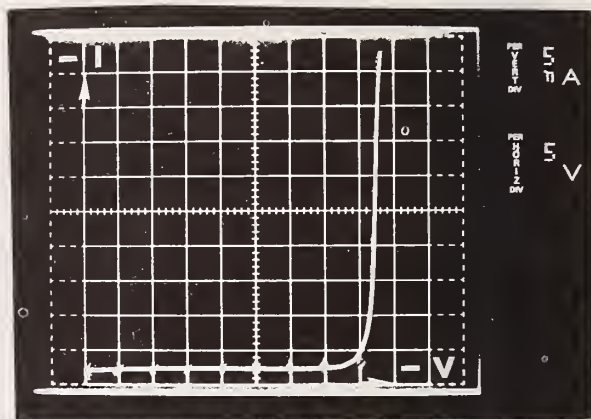
Standardization Activities - Further study was made of the results of the partially completed round robin on four-probe measurement of resistivity of silicon epitaxial layers deposited on substrates of opposite conductivity being conducted in cooperation with the Resistivity Section of ASTM Committee F-1 on Electronics. The conclusion was reached that the results to date are not adequate to support a precision statement in the test method. Plans for resuming the round robin were prepared and presented at the September meeting of the Committee.

(J. R. Ehrstein and F. H. Brewer)

Proposed methods for providing resistivity standards to the semiconductor device industry (NBS Tech. Note 560, pp. 10-11) were also discussed at the September meeting of the Committee. As a result of the discussion a modified collaborative reference program has been given primary consideration as the most useful vehicle for providing standards. In such a program a consensus definition of standard values is arrived at through a multipass exchange of material between NBS and the other participants. The consensus is biased in the direction of the NBS data by virtue of the fact that NBS measures the circulated specimens immediately before each shipment to another participant. In addition, if feasible, replicate specimens are to be provided to each participating laboratory during the program. Such replicates would provide each laboratory with a link to the consensus specimens at times when those specimens are in circulation elsewhere.

A program of this sort would be expected to provide information on the extent of deterioration of standards samples with use and an understanding of typical "between/within" measurement errors [1] to be experienced in using resistivity standards, as well as to identify changes in measurement conditions that might be desirable. It is anticipated that this means of achieving resistivity standards would be succeeded by a less cumbersome one, such as one involving the use of standard reference materials with certified resistivity values, at some later date. At present, consideration is being given to detailed experimental design, various experimental safeguards, possible cost to participants, and the general logistics of such a program. (J. R. Ehrstein)

Figure 1. Typical reverse current-voltage characteristic for a 0.5-mm diameter silicon diode prepared for capacitance-voltage measurements. (The wafer was diffused for 63 min at 1038°C with an oxidized boron nitride source and an ambient of 99 percent nitrogen, 1 percent oxygen with a flow rate of about 2500 cm³/min. The wafer was initially doped with phosphorous at a level of about 3×10^{14} cm⁻³. The junction depth was 1.05 μm and the boron surface concentration was 5×10^{20} cm⁻³.)



Capacitance-Voltage Method – The search continued to discover the origin of the linear defects observed on low quality diodes (NBS Tech. Note 702, p. 8). A 1.8-Ω·cm *n*-type silicon wafer, fully sliced and polished by the manufacturer, was used to fabricate an array of *p-n* junctions. More than 90 percent of the diodes in the finished array exhibited reverse breakdown voltages of 50 to 70 V. This suggested that the oxidation, photolithography, and diffusion processes were not the cause of the previously observed linear defects.

A second group of similar, sliced and polished, 1.8-Ω·cm *n*-type silicon wafers was then subjected to various mechanical treatments to investigate the effect of in-house preparation on final diode yield. These treatments included lapping, mechanical polishing, and chem-mechanical polishing. Following these treatments diode arrays were fabricated as before. Wafers which were mechanically polished or lapped and mechanically polished but which had no final chem-mechanical polish treatment exhibited an average breakdown voltage of about 12 V. The wafer which had been chem-mechanically polished after lapping exhibited an average breakdown voltage of 42 V. A current-voltage characteristic typical of diodes from this wafer is shown in figure 1. Leakage currents to the point of breakdown in these diodes are usually less than 2 nA at room temperature. In addition, a diode array that exhibited an average breakdown voltage of 71 V was fabricated on a 2.9-Ω·cm *n*-type silicon wafer which had been sawed as well as polished in-house. Therefore, it could be concluded that lapping and mechanical polishing introduced defects which could then be removed by chem-mechanical polishing.

Since the 12-Ω·cm *n*-type wafers upon which the linear defects were originally observed had also been chem-mechanically polished in-house, the origin of the defects in these wafers is still unidentified. An experiment to see if the linear defects were inherent in the 12-Ω·cm material is currently in progress on a third group of specimens. A wafer of the 12-Ω·cm *n*-type silicon in which the defects were first observed, a wafer of the 2.9-Ω·cm *n*-type silicon discussed above, and a wafer of

RESISTIVITY

1.4- Ω ·cm *n*-type silicon are being processed from sawing to diffusion in preparation for observation and electrical measurements.

(R. L. Mattis, T. F. Leedy, and M. Cosman)

Attention was given to factors which may be used to correct capacitance-voltage data for fringing around the edge of the diode, diffusion tails into the region being profiled, and back depletion into the diffused layer. Some of the things considered included a published edge correction applicable to Schottky barrier diodes [2], the error in computed doping density that results from error in the measurement of capacitance, voltage, or diode area of an ideal abrupt junction, and the effect of making the measurement in a junction which is not abrupt but which can be approximated by an exponential doping distribution over the region of interest. When the edge correction was applied to existing C-V data the result was often a flattening of the doping density versus depth profiles. An edge correction would therefore appear to be suitable, and one applicable to diffused diodes is being sought.

(R. L. Mattis)

Difficulties have been experienced in the past getting a high degree of agreement between resistivity values of bulk silicon slices as measured by the four-probe technique and as derived from capacitance voltage measurements. Therefore, five sets of *n*-type silicon wafers with radial resistivity gradient of 5 percent or less at half radius were obtained for detailed comparison of the capacitance-voltage and four-probe methods for measuring resistivity. Sets of 20 or more lapped wafers with nominal resistivity of 0.2, 0.3, 1.5, 4, and 8- Ω ·cm are being processed. Three wafers from each set have been visually inspected, profiled along perpendicular diameters by the four-probe method, and chem-mechanically polished on one side prior to fabrication of diode arrays.

(R. L. Mattis and D. R. Ricks)

Spreading Resistance Methods — A study of probe damage on silicon wafers with the scanning electron microscope continued. Because of general past difficulties with bulk silicon specimens both with and without gold coatings, an epitaxial specimen was tried instead. A *p*-type epitaxial layer of about 0.1- Ω ·cm on about a 10- Ω ·cm *n*-type substrate was used; electrical contact was made to the epitaxial layer. Moderate resolution photographs of 5000 X were obtained, less than the best magnification yet obtained with bulk silicon, but better than results generally experienced with bulk silicon. In general, the epitaxial specimen allowed the identification of the probe damage locations with greater ease than was generally true on bulk specimens. Difficulties with apparent surface contamination build-up were not eliminated, however.

(J. R. Ehrstein)

Plans: The study of current and probe-force dependence of four-probe resistivity will continue on wafers previously measured after the surfaces are vapor etched. The detailed analysis of results to date will continue, and an attempt to sort out the current level dependence from the dependence on the order of current level sampling will be made. Work will be resumed on the use of the surface photovoltage effect in an attempt to

RESISTIVITY

relate surface treatment procedures to changes in subsurface damage and in measured resistivity.

The round robin on measurement of resistivity of epitaxial layers by the four-probe method will be resumed. Details related to the establishment of a functional program for providing silicon resistivity standards to the industry will be investigated.

The experiment currently in progress to identify the source of the observed linear defects in a wafer used to fabricate diode arrays for C-V measurements will be completed. Capacitance-voltage and four-probe resistivity values will be compared for slices from the five sets of *n*-type silicon wafers. Consideration will be given to the suitability of shallow diffusions, Schottky barriers, and metal-oxide-semiconductor structures for measuring doping density in thin layers by C-V methods.

3.2. GOLD-DOPED SILICON

Objective: To characterize *n*- and *p*-type silicon doped with gold and to develop a model for the energy-level structure of gold-doped silicon which is suitable for use in predicting its characteristics.

Progress: Resistivity measurements on gold-doped *n*-type silicon wafers and diffusions of gold into *p*-type silicon wafers were made as scheduled and analyzed. Several short-time diffusions and annealing treatments were made to study effects due to interstitial gold and precipitation of gold, respectively. Additional preliminary measurements of carrier lifetime in gold-diffused wafers were made by the surface photovoltage method.

Resistivity Measurements - Resistivity and Hall effect measurements were made at room temperature ($25 \pm 1^\circ\text{C}$) on Hall bars cut from 5-, 80-, and 400- $\Omega\cdot\text{cm}$ *n*-type wafers that had been diffused with gold at 850, 950, 1050, 1150, and 1250°C and from 2200- $\Omega\cdot\text{cm}$ *n*-type wafers diffused at 950, 1050, 1150, and 1250°C. In all cases except the 5- $\Omega\cdot\text{cm}$ wafer diffused at 850°C, the gold concentration exceeds the shallow donor concentration. As the gold concentration is increased, the resistivity is expected to reach a maximum and then decrease. Shortly before the maximum the specimens become *p*-type. At large values of gold concentration the resistivity should approach a constant value characteristic only of the gold impurity. The resistivity maximum should occur at the intrinsic value where the product of electron concentration and mobility is equal to the product of hole concentration and mobility and, except for possible differences in mobility, be independent of the resistivity of the wafer before gold is added.

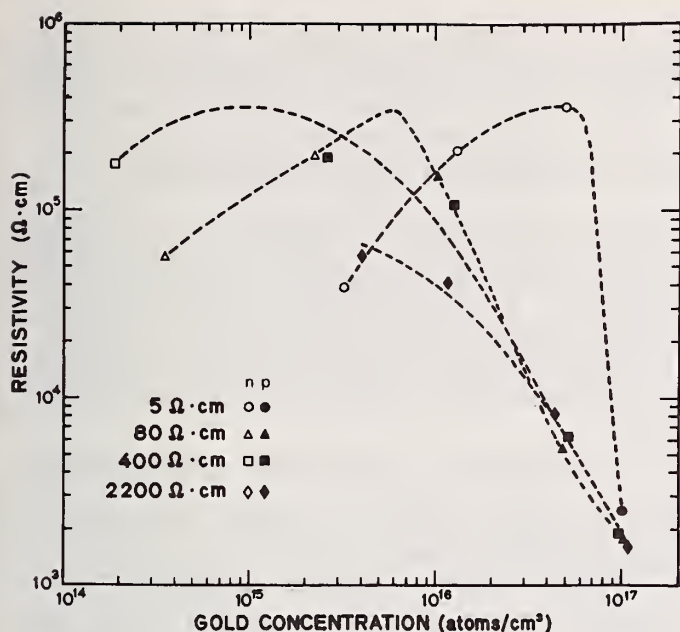


Figure 2. Resistivity as a function of gold concentration in initially *n*-type silicon. (Resistivity of the specimens prior to gold doping is given. Open symbols represent specimens which remained *n*-type after gold diffusion; solid symbols, specimens which were converted to *p*-type by the addition of gold. The dashed curves indicate the form of the relationship between resistivity and gold concentration required by the existence of a common maximum as discussed in the text. Error bars are not indicated. The standard deviation of the gold determination is estimated to be about 10 percent. Resistivity values are reproducible within about 10 percent.)

The measured resistivity, shown in figure 2, is generally consistent with theoretical expectations although it does not agree in a number of important details. The dashed lines associated with the data points suggest the form the resistivity-concentration curves would have to take in order to reach a common resistivity maximum near the value of about $3.5 \times 10^5 \Omega \cdot \text{cm}$ calculated for a temperature of 25°C (intrinsic carrier concentration $1.10 \times 10^{10} \text{ cm}^{-3}$, electron mobility of $1300 \text{ cm}^2/\text{V}\cdot\text{s}$, and hole mobility of $500 \text{ cm}^2/\text{V}\cdot\text{s}$). The differences in shapes of these curves, the poor fit of the data for the $400\text{-}\Omega \cdot \text{cm}$ specimens, and the *n*-type nature of the $5\text{-}\Omega \cdot \text{cm}$ specimen diffused at 1150°C (which appears at the maximum) all are indicative of either experimental or interpretative difficulties. The experimental data were taken with a newly fabricated specimen holder designed to provide improved means for controlling and measuring the specimen temperature which is a most important consideration when measuring specimens with near-intrinsic resistivity, but this does not preclude the existence of other experimental problems.

Perhaps even more significant is the fact that the resistivity at the largest gold concentrations approaches a value lower by at least an order of magnitude from that predicted by any model examined to date. The value approached is consistent with the resistivity measured on *p*-type wafers which had about the same value of resistivity at a gold concentration of 10^{17} atoms per cubic centimeter (NBS Tech. Note 702, pp. 9-10). Evidently the same mechanism is affecting the resistivity in both types of specimens. (W. R. Thurber, A. W. Stallings, and W. M. Bullis)

Specimen Preparation — Gold diffusions were completed on sets of *p*-type wafers with initial resistivity of 0.5, 1000, and 2000 $\Omega \cdot \text{cm}$. Gold concentrations were determined by neutron activation analysis at the

NBS reactor facility on portions of the wafers diffused at 850, 950, and 1050°C. Wafers diffused at 1150 and 1250°C have been lapped and cut in preparation for analysis. Four 10-Ω·cm *p*-type wafers were diffused at 1250°C for times of 8, 16, 32, and 64 hours to determine if foreign impurities are introduced during the high temperature diffusions.

To examine the effect of interstitial gold on the electrical properties of silicon, diffusions of short duration were done at 950 and 1150°C in both *n*- and *p*-type 2000-Ω·cm wafers. A study of possible gold precipitation was begun in which two slices, previously diffused, were lapped and their rims sandblasted to remove regions of high gold concentration. One slice was annealed at a higher temperature than the original diffusion and one at a lower temperature.

(W. R. Thurber, A. W. Stallings, J. Krawczyk, and M. Cosman)

Carrier Lifetime Measurements — Measurements of carrier diffusion length by the surface photovoltage method on the etched surface of a Hall bar cut from a 10-Ω·cm *p*-type wafer with a gold concentration of 4.9×10^{14} atoms per cubic centimeter gave a diffusion length of 10 μm. The value of about 30 ns calculated for the minority carrier lifetime is consistent with the capture cross section of electrons on the positively charged gold donor center reported by Fairfield and Gokhale [1]. Preliminary measurements were also made on a portion of a 10-Ω·cm *p*-type wafer with a gold concentration of 2.9×10^{16} atoms per cubic centimeter. Although a diffusion length of about 1 μm was obtained, additional measurements are needed to confirm this value as the degree of reproducibility that can be achieved in measuring such short diffusion lengths has not been established. The calculated lifetime for a 1 μm diffusion length is 0.3 ns, somewhat shorter than would be obtained from published values of capture cross-sections.

(W. R. Thurber, W. E. Phillips, and W. M. Bullis)

Plans: Electrical measurements will be made on Hall bars cut from the 0.5-, 10-, 1000-, and 2000-Ω·cm gold-diffused *p*-type wafers. Data will also be obtained on the wafers which have been diffused to study interstitial and precipitated gold. Additional material will be selected for diffusion.

Study of the application of the surface photovoltage methods to the measurement of short carrier lifetimes will continue. Additional carrier diffusion length measurements will be made by the surface photovoltage method on many of the Hall bars used for electrical measurements. The apparatus will be further improved and studies of the reproducibility that can be obtained will be undertaken.

Models for the recombination of carriers through the gold centers will be studied, and available information on capture cross sections will be examined further. Search for a suitable model to explain the electrical behavior of heavily gold-doped silicon will continue.

3.3. INFRARED METHODS

Objective: To study infrared methods for detecting and counting impurity and defect centers in semiconductors, and, in particular, to evaluate the suitability of the infrared response technique for this purpose.

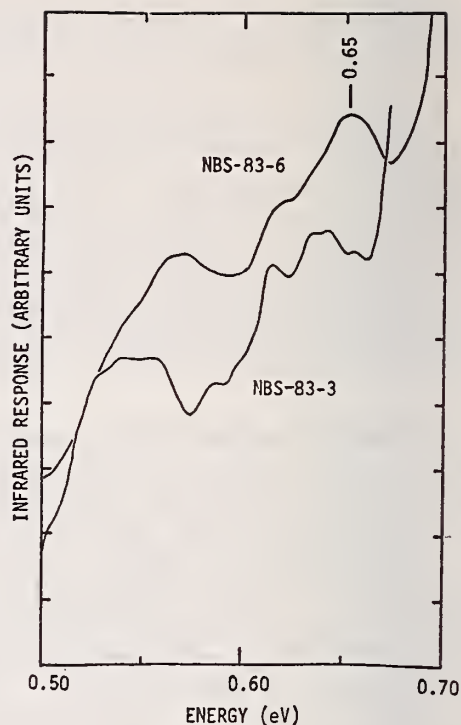
Progress: The infrared response (IRR) technique was used to study nine germanium diodes; the presence of lithium precipitate clusters was tentatively identified in two diodes. Initial IRR measurements on three lithium-drifted silicon detectors, two of which had been subjected to radiation damage, revealed features at energies associated with divacancies, the vacancy-oxygen pairs, and lithium precipitates. A second cryostat has been constructed for use with this technique, and the system for converting the analog output of the IRR system into digital form was put into use.

Infrared Response Measurements on Germanium - The infrared response (IRR) of nine lithium-drifted germanium diodes was measured during this quarter. One diode that was of special interest was NBS 83-6, fabricated from a specimen of the same crystal as were NBS 83-3 and NBS 83-4 (NBS Tech. Note 598, pp. 14-15). This specimen had been thermally-diffused with lithium at 390°C for 15 min (depth \sim 750 μ m) and was stored at room temperature for several months prior to lithium drifting. The finished detector exhibited such severe carrier trapping that no peaks were observed in a ^{60}Co gamma-ray spectrum (1173.2- and 1332.5-keV gamma rays) despite the fact that an electric field of several hundred volts per centimeter could be applied to the device. In figure 3 the IRR spectrum obtained from NBS-83-6 is compared with that obtained from NBS-83-3 which is considered to be an example of good-quality germanium. It has been suggested by Armantrout [1] that the formation of lithium precipitate clusters can introduce bands of energy levels below the conduction band due to the strain induced in the crystal lattice. Based on results of previous lithium precipitation measurements [2], it is quite likely that considerable lithium precipitation occurred because of the prolonged storage at room temperature of NBS-83-6 prior to drifting. The bands of levels mentioned above might then account for the "smearing" of the spectrum of NBS-83-6 relative to that of NBS-83-3 shown in figure 3. That lithium precipitates have a large trapping cross-section for holes [1] might also account for the severe degradation in charge collection observed in NBS-83-6. It is to be noted that the IRR spectrum of NBS-83-6 bears some resemblance to that of NBS-113, a specimen of high-purity germanium doped with approximately 10^{11} gold atoms per cubic centimeter (NBS Tech. Note 702, pp. 12-13); however, the maximum in the spectrum at 0.66 eV does not appear in the spectrum for NBS-83-6.

Subsequently, another specimen, NBS-74, one of the 85 crystals of various origins collected for the study of germanium problems, was found to exhibit an IRR spectrum similar to that of NBS-83-6. This specimen showed poor charge collection as a Ge(Li) detector, both at this and the originating laboratory; the IRR response suggests that the reason for poor detector quality is the formation of lithium precipitate clusters.

INFRARED METHODS

Figure 3. Infrared response spectra of two lithium-drifted, germanium gamma-ray detectors.



Two other diodes, NBS-302 and NBS-303, that were characterized by electron trapping at the originating laboratory were observed to have a strong IRR peak at 0.50 eV indicative of the lithium-defect trap. This trap was shown previously to be preferential for electrons [1].

(A. H. Sher, W. J. Keery, and H. E. Dyson)

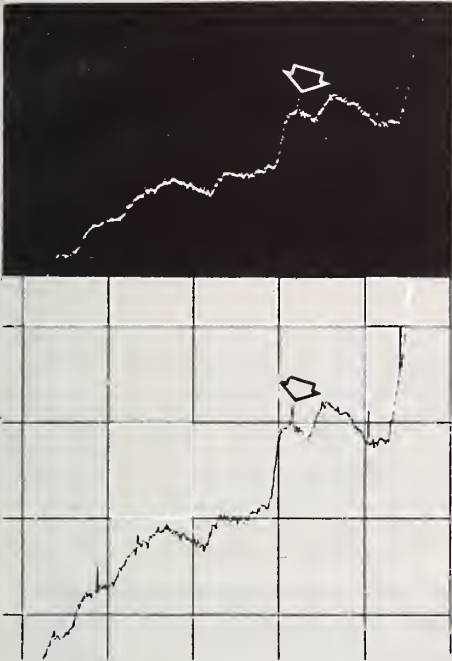
To aid in the intercomparison of IRR spectra from diodes of different sensitive volumes, the first of a series of experiments was performed on specimen NBS-83-12. The IRR was measured after an initial drifting period and then measured again after further lithium-drifting. Using a 1-mm thick germanium filter window, an increase in the IRR signal of approximately 30 percent was observed for a 20 percent increase in sensitive volume.

(E. A. Simmons)

The construction of a second cryostat for use in IRR measurements has been completed. This cryostat has the same features as the one currently in use (see NBS Tech. Note 555, p. 17) but has both a larger charge of molecular sieve and a larger dewar to increase the holding time of diodes under study. With the new cryostat an increased number of diodes of the same type can be studied; further, the amount of time required to prepare a cryostat for use with diode configurations that require special mounts is reduced.

(W. J. Keery and G. P. Spurlock)

Figure 4. Comparison of the digital form of an infrared response spectrum as displayed on the oscilloscope of a multi-channel analyzer system (top) with a directly obtained strip chart recording of the same spectrum (bottom).



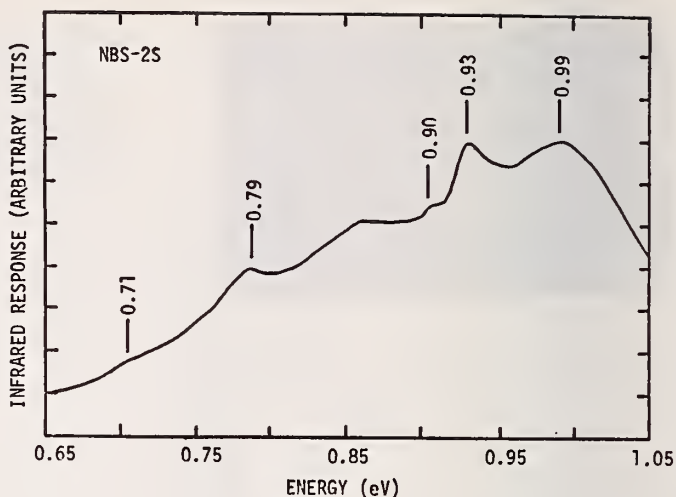
In figure 4 the digital form of an IRR spectrum photographed from the oscilloscope display of the multichannel analyzer obtained using the equipment previously described (NBS Tech. Note 702, pp. 12-13) is compared with an analog strip chart recording of the same data. The digital information faithfully reproduces the analog form as can be seen from the noise spikes indicated by arrows. Once stored in the multichannel analyzer, the spectrum can be printed out in hard copy form, punched onto paper tape for computer analysis or storage, plotted out by x-y point plotter, or displayed on the oscilloscope. (W. J. Keery)

Several specimens from germanium crystal NBS-83 have been prepared for neutron irradiation and subsequent IRR measurement. Some specimens were untreated, some were lithium-diffused, and others were compensated by lithium drifting. (A. H. Sher and Y. M. Liu)

The nearly completed initial phase of the IRR study of germanium crystals has shown that the improved IRR technique can be used to obtain information on the energy levels of known defects and impurities introduced into germanium. This phase included measurements of the infrared response and iron-doped copper-, gold-germanium, and of specimens known to contain thermally-generated acceptors, lithium-defect centers, and lithium precipitates. IRR measurements on neutron-irradiated germanium specimens remain to be done to complete this initial phase.

The second phase, which has been carried on concurrently to some extent with the initial phase in order to gain some understanding of the

Figure 5. Infrared response spectrum of a lithium-drifted, silicon detector after neutron irradiation.



experimental results obtained thus far, consists of a detailed study of the literature on photoconductivity measurements on germanium and silicon containing known impurities and defects and experimental investigation of the effects of infrared quenching, crystal surface condition, and filter bandwidth on photoconductivity. This phase of the study is intended to provide a deeper understanding of the measurement method in order that some general conclusions can be drawn regarding the causes of poor quality in semiconductor crystals used in the fabrication of nuclear radiation detectors.

(A. H. Sher)

Infrared Response Measurements on Silicon — Measurements of IRR on lithium-drifted silicon nuclear radiation detectors of commercial origin were begun this quarter. These detectors are mounted in metal annular rings so that unlike the case for the germanium detectors, infrared radiation must be directed through the thin gold contact to the *p*-type region. Thus, in addition to the effects of this thin gold electrode that is about 15 nm thick, the applied bias on the detector should have a considerable effect on the observed IRR spectrum because of its effect on the thickness of the insensitive, undepleted region behind the *p*-contact. Such effects have been observed on a pair of detectors fabricated from the same crystal, one electron-damaged and the other unirradiated. Work is proceeding on the interpretation of these effects. The IRR spectrum of NBS-2S, a lithium-drifted detector subjected to neutron irradiation at a fluence of about 10^{11} cm⁻², taken at 100 K with a 0.14-mm thick silicon filter window on the cryostat is shown in figure 5. The bandedge peak in silicon was found to be at 1.17 eV. Features whose energies are identified in figure 5 can be tentatively linked to the defects listed in table 1. A peak at approximately 0.59 eV (corresponding to one-half the bandgap energy) is also observed as in the case of germanium (NBS Tech. Note 555, p. 25).

(A. H. Sher, W. J. Keery, and Y. M. Liu)

INFRARED METHODS

Table 1 - Features in Neutron-Irradiated,
Lithium-Drifted Silicon Detector

Feature	Defect State	Origin
0.99 eV	$E_C - 0.17 \text{ eV}$	vacancy-oxygen pair ^a
0.93 eV	$E_V + 0.24 \text{ eV}$	divacancy ^b
0.90 eV	$E_V + 0.27 \text{ eV}$	lithium precipitate ^c
0.79 eV	$E_C - 0.38 \text{ eV}$	divacancy ^b
0.71 eV	$E_V + 0.45 \text{ eV}$	lithium precipitate ^c

^a Corbett, J. W., Electron Radiation Damage in Semiconductors and Metals, Suppl. 7, *Solid-State Physics*, (Academic Press, New York, 1966).

^b Konozenko, I. D., Semenyak, A. K., and Khivrich, V. I., Radiation Defects Created by Co^{60} γ -Rays in *p*- and *n*-Type Silicon of High Purity, *Phys. Stat. Sol.* 35, 1043-1052 (1969).

^c Smirnova, I. V., Chapnin, V. A., and Vavilov, V. S., Radiation Defects in Lithium-Doped Silicon, *Sov. Phys. - Solid State* 4, 2469-2474 (1962-63).

Plans: An intensive review of photoconductivity literature for germanium and silicon will be begun. The study of the IRR of diodes fabricated from the collection of 85 germanium crystals now on hand will continue at an increased rate, and the results will be correlated with measured detector characteristics. The study of the IRR of silicon detectors will also proceed. Efforts to extend the use of the IRR technique to transistors and diodes will resume.

3.4. SPECIFICATION OF GERMANIUM

Objective: To measure the properties of germanium crystals and to correlate these properties with the performance of germanium gamma-ray detectors in order to develop methods for the early identification of crystals suitable for fabrication into lithium-compensated gamma-ray detectors.

Progress: Principal effort during this quarter was directed toward the continuing study of the infrared response (IRR) technique. This work is reported in the section on infrared methods (see Section 3.3). The operating characteristics of several Ge(Li) detectors were measured in conjunction with the infrared response study in order to obtain information to aid in the interpretation of the IRR method. Work has resumed on

SPECIFICATION OF GERMANIUM

collection of the bibliography of publications relating to Ge(Li) detector technology that have appeared since January 1, 1969.

(A. H. Sher, W. J. Keery, and H. E. Dyson)

Plans: The Ge(Li) detector bibliography will be completed and preparations will be instituted for its publication. Work on Ge(Li) detectors will be carried out in cooperation with the Germanium Section of ASTM Committee F-1 on Electronics; the exact nature of this effort has not yet been decided upon by the Section. The results of the study of infrared response will continue to be applied to the measurement of germanium quality.

3.5. REFERENCES

3.1. Resistivity

1. Mandel, J., Repeatability and Reproducibility, *Materials Research and Standards* 11, No. 8, 8-15, 52 (1971).
2. Copeland, J. A., Diode Edge Effect on Doping-Profile Measurements, *IEEE Trans. Electron Devices* ED-17 404-407 (1970).

3.2. Gold-Doped Silicon

1. Fairfield, J. M., and Gokhale, B. V., Gold as a Recombination Centre in Silicon, *Solid-State Electronics* 8, 685-691 (1965).

3.3. Infrared Methods

1. Armantrout, G. A., Infrared Evaluation Techniques for Ge(Li) Detectors, *IEEE Trans. Nucl. Sci.* NS-17 No. 2, 16-23 (1970).
2. Sher, A. H., Croll, W. K., and Thurber, W. R., Determination of Oxygen in Germanium Below 20 Parts per Billion by Measurements of Lithium Mobility and Precipitation, *Anal. Chem.* 43, 1831-1834 (1971).

4. METHODS OF MEASUREMENT FOR PROCESS CONTROL

4.1. DIE ATTACHMENT EVALUATION

Objective: To evaluate methods for detecting poor die attachment in semiconductor devices with initial emphasis on the determination of the applicability of thermal measurements to this problem.

Progress: Work reported previously (NBS Tech. Notes 598, pp. 18-20, and 702, pp. 15-17) indicated that a measurement of transient thermal response of a semiconductor diode, using a pre-determined heating power pulse width, is more sensitive to the presence of voids in the die attachment material between the semiconductor chip and header than is a measurement of the thermal resistance or steady-state thermal response of the diode. The results reported showed that a 10-percent circular void in the chip bonding area is the lower limit in void size that can be detected by using the transient thermal response technique in the particular device structure studied. It was also found that the spread in thermal response of a group of devices with 20-percent void areas was significantly larger than in that of devices with 40-percent and 10-percent void areas.

Measurements of steady-state thermal response and transient thermal response for heating-power pulse widths ranging from 5 to 100 ms were made on several groups of diodes bonded to TO-5 headers with dimples ultrasonically machined into the bonding surface to provide voids of known size. Group K devices consisted of diode chips bonded to TO-5 headers with off-center 15-mil (0.37-mm) diameter dimples. Group L and M devices consisted of bare silicon and gold backed diode chips, respectively, bonded to TO-5 headers with 20-mil (0.51-mm) diameter dimples. Ten control devices without voids were bonded with each group of devices with the various size voids. The spread in thermal response of the Group L devices with the 20-percent void areas was significantly improved over the spread reported previously for Group H devices which had the same 20-percent dimple area in the header (NBS Tech. Note 702, pp. 15-16). This result is in accord with the previous finding that the Group H devices were not properly bonded and that some had void areas larger than the dimple.

The results obtained on the most recently prepared groups as well as on two earlier groups are summarized in table 2. The first group of entries gives the junction-to-case temperature difference measured under steady-state conditions for the control diodes [ΔT_{ss} (controls)] and the diodes with voids [ΔT_{ss} (voids)]. A heating current of 300 mA was used. The third line is the increase in the average junction-to-case temperature difference of the voided devices over that of their controls expressed as a percentage of the latter. The range given is one sample standard deviation. The second group of entries gives the junction-to-case temperature difference measured after a 10-ms long power pulse for the control diodes [ΔT_t (controls)] and the diodes with voids [ΔT_t (voids)].

DIE ATTACHMENT EVALUATION

TABLE 2 - Summary of Results of Junction-to-Case Temperature Difference Measurements

Lot No.	J	K ^a	L	M	I ^d
ΔT_{ss} (controls) (°C)	15.53±0.73	15.06±0.37	15.58±0.48	16.04±0.39	15.02±0.52
ΔT_{ss} (voids) (°C)	15.91±0.57	15.71±0.40 ^b	16.93±0.35 ^c	18.06±0.62 ^c	16.69±0.59 ^c
% increase	2.4 ±6.0	4.3 ±3.6	8.7 ±3.8	12.6 ±4.6	11.1 ±5.3
ΔT_t (controls) (°C)	12.01±0.90	12.62±0.72	11.74±0.49	14.62±0.67	11.33±0.55
ΔT_t (voids) (°C)	13.26±1.16	13.83±0.73 ^b	15.66±0.63 ^c	18.98±1.19 ^c	15.22±0.63 ^c
% increase	10.4±12.3	9.6 ±8.2	33.4 ±7.0	29.8 ±9.5	34.3 ±7.6
% difference (t-ss)	333	123	284	137	209
Lot J	15-mil (0.37-mm) diameter (10%) void area				
Lot K	15-mil (0.37-mm) diameter (10%) void area, off-center				
Lot L	20-mil (0.51-mm) diameter (20%) void area				
Lot M	20-mil (0.51-mm) diameter (20%) void area, gold-backed				
Lot I	29-mil (0.74-mm) diameter (40%) void area				

^a $t_{meas.} = 30 \mu s$

^b 13 diodes

^c 9 diodes

^d power-pulse width = 9 ms

A heating current of 800 mA was used. The third line of this group is the increase in the average junction-to-case temperature difference of the voided devices over that of their controls expressed as a percentage of the latter. Again, the range given is one sample standard deviation. The last line of the table gives the difference between the percent increase obtained for transient response measurement and that obtained for steady-state response measurements expressed as a percentage of the latter. This quantity represents the percent increase in sensitivity to voids of transient response over that of steady-state response. Except where otherwise noted each sample group consisted of 10 diodes and the thermal response was measured 50 μs after the termination of the power pulse.

The percent increase in sensitivity to voids of transient thermal response over the steady-state thermal response measurements varied from 123 percent to 333 percent. It should also be noted that in the case of the devices with the 10 percent void areas (Columns J and K), the increase in average steady-state thermal response of the devices with voids over that of their controls ranged from 2.4 to 4.3 percent. This increase is of the same order as the sample standard deviation of the controls for these groups and therefore does not yield a useful indication of the presence of voids. For the transient thermal response measurements it was

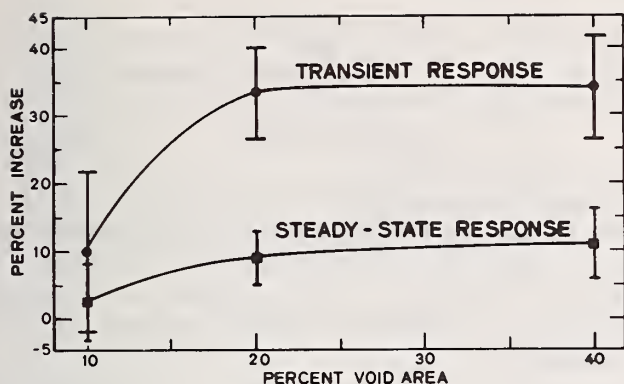


Figure 6. Percent increase in average junction-to-case temperature difference of diodes with voids over that of their respective controls measured under steady-state and transient conditions as a function of percent void area in the diode die attachment. (Error bars indicate one sample standard deviation).

found that for half of the diodes with voids, the measured junction-to-case temperature difference fell within the scatter obtained on the controls, while the other half showed significantly larger values.

The average percent increase in steady-state and transient thermal response of the devices with voids over their respective controls is shown in figure 6 as a function of percent void area. For void areas of 20 and 40 percent, the increase in both steady-state and transient thermal response of the devices with voids over their respective controls is nearly the same, although the percent increase in transient thermal response over the controls is three times that of the steady-state thermal response. This implies that a given increase in electrically measured thermal response may be indicative of a wide range of void sizes. Also, the data presented indicate that, at least for this particular device, measuring steady-state thermal response (or thermal resistance) would not be an acceptable industrial screening technique to cull out devices with various size voids due to the low sensitivity of the technique, while measuring the transient thermal response for a particular heating power pulse would. Although a 10 percent increase in thermal resistance might appear to be acceptable from a thermal standpoint, a 20- to 40-percent void area might be totally unacceptable from a thermal fatigue or thermal shock viewpoint.

A study was undertaken to determine whether increasing the low level measuring current would decrease the non-thermal switching effects such that the temperature sensitive parameter could be measured sooner, thus increase its sensitivity to voids. The low level measuring current is that current which is applied after the termination of the heating power pulse and during which time the temperature sensitive parameter is measured. It was found that by increasing the measuring current from 1 mA to 5 mA, the temperature sensitive parameter could be measured 25 μ s after the termination of the heating power pulse instead of 50 μ s. Measurements made on the group M, gold-backed silicon chip devices, at both 25 and 50 μ s indicated that no general increase in sensitivity was gained by decreasing the delay time in measuring the temperature sensitive parameter; in fact,

DIE ATTACHMENT EVALUATION

the average sensitivity decreased slightly. The reason for this decrease in sensitivity appears to be the slow rate of cooling of these devices between 10 and 50 μ s combined with the wide variation in the rate of cooling of the devices with voids. (F. F. Oettinger and R. L. Gladhill)

A theoretical study was undertaken to ascertain the limitations of thermal response techniques for detecting poor die adhesion in the devices under investigation. A tool that is being considered for use in this study is the TRUMP [1] thermal analysis program. This program is expected to allow both transient and steady-state temperature distributions to be calculated for multidimensional systems.

(W. E. Phillips and F. F. Oettinger)

Plans: Measurements of steady-state and transient thermal response on diodes with two controlled voids, having a total void area of 20 percent will be made to investigate the dependence of thermal response on the details of the void geometry. Measurements will also be made on diode chips bonded to solid-steel TO-5 headers. These measurements are intended to test the assumption that the transient thermal response for a given chip size and power dissipation, measured under conditions such that the heating power pulse width is less than the case time constant, is relatively independent of the case thermal resistance. A study will be undertaken to determine to what extent the transient thermal response measurement procedure can be simplified and made less time consuming for use as an industrial screen. The theoretical study to determine the limitations of thermal response techniques for detecting poor die adhesion in the devices under investigation will continue. Experiments to apply the transient thermal response technique to include transistors with poor die adhesion will be initiated.

4.2. WIRE BOND EVALUATION

Objective: To survey and evaluate methods for characterizing wire bond systems in semiconductor devices and where necessary to improve existing methods or develop new methods in order to detect more reliably those bonds which eventually will fail.

Progress: Additional calculations have been carried out to examine the problem of thermal-expansion-induced wire bond-loop flexing in more detail. Application of a minimum loop-height specification based on the results of these calculations to a production run of transistors has resulted in a dramatic decrease in failure due to slow thermal cycling. Progress was made in adapting ribbon-wire bonding techniques to a production environment. Work was resumed on the study of bonding tool motion during bonding by means of a capacitor microphone. This work is directed toward the eventual development of an in-process control technique for

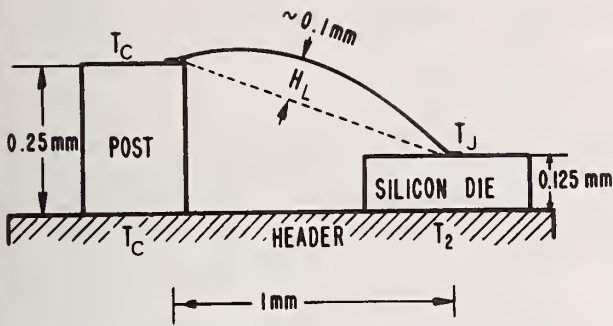


Figure 7. Schematic representation of device structure assumed in calculation of wire-bond flexure.

the evaluation of bonds. Work on evaluation of the destructive, double-bond, pull test has resumed with the continuation of experiments to test the effects on the measured pull strength of single-level bond pairs of variation in pull rate, pull angle, and hook position. Results of a second series of tests to determine the effect of variations in bond angle on the measured pull strength of single-level bond pairs pulled vertically at the center of the loop did not agree with the results obtained previously.

Bond Failure from Slow Thermal Cycling — Transistor failure under conditions of thermal cycling at slow rates has been traced to wire fatigue resulting from repeated thermal-expansion-induced wire flexing as discussed previously (NBS Tech. Note 598, pp. 24-25). Additional calculations of wire flexure have been carried out to examine this problem in greater detail.

The analysis was made specifically for the 1-mil (25- μ m) diameter post-to-die aluminum wire interconnection in a 500-mW, 50-mA silicon transistor in a TO-18 can with post and header of the usual iron-nickel-cobalt alloy, but it is generally applicable to other devices with similar current and power ratings. The device under study is shown schematically in figure 7. It was assumed that all heat was generated as a result of power dissipation in the device; Joule (I^2R) heating in the wire was assumed to be insignificant at the relatively low current levels in the device. Based on manufacturer's specifications and empirical data and for an ambient temperature of 23°C the junction temperature was taken as $T_J = 23 + 0.314 P$; the temperature under the die, as $T_2 = T_J - 0.012 P$; and the case temperature, as $T_C = 23 + P^{0.7}$ where the power dissipation, P , is in milliwatts.

Thermal expansion was assumed to be linear over the test range and the expansion coefficients were taken as $2, 5, \text{ and } 24 \times 10^{-6}/^\circ\text{C}$ for silicon, iron-nickel-cobalt alloy, and aluminum, respectively. The header expansion was assumed to be due only to the change in case temperature; local heating under the die only increases internal header stress. Die expansion was calculated on the basis of a uniform temperature taken to be the arithmetical average of the top and bottom temperatures. The

change in length of the various elements is then:

$$X(P) = X_0 [1 + \alpha(T - 23)],$$

where X_0 is the length of the element at ambient temperature, α is the thermal expansion coefficient of the material, and T is the temperature of the element, a function of the power dissipation, P . The wire is attached at points on the post and the die. The bond-to-bond distance, L , is given by:

$$L = [d^2 + (Y - Z)^2]^{1/2},$$

where d is the bond-to-bond distance in the plane of the header, Y is the post height and Z is the die height.

The temperature distribution along the wire was accounted for with the assumption that the temperature decreased exponentially from T_J to T_C with a characteristic length, λ :

$$T(x) = T_C + (T_J - T_C) \exp(-x/\lambda),$$

where x is the coordinate along the wire in the direction from the die to the post. If $\lambda = S_0/2$, the length of the wire is:

$$S = S_0 [1 + \alpha_{Al}(0.57T_C + 0.43T_J - 23)].$$

The prefactors for T_C and T_J are changed if other values of λ are selected.

The flexure can be defined as the change in loop height:

$$\Delta H_L = H_L - H_{L0}.$$

The functional relationship between loop height and the lengths S and L depends on the shape of the wire loop. Calculations were made for two cases; bending moments in the wire were neglected. If the wire loop is in the form of an arc of a circle, the loop height is given approximately by:

$$H_L = [3(3S + 5L)(S - L)]^{1/2}/8,$$

If the loop is assumed to retain its circular shape during flexing, this expression is appropriate for calculations before and after flexing. The calculation is made by selecting a value for H_{L0} and computing S_0 to obtain the initial condition. Then S , L , and ΔH_L are computed for various values of P to obtain the flexure as a function of power dissipation. The results for $H_{L0} = 50, 100, \text{ and } 250 \mu\text{m}$ are identified by semicircular symbols in figure 8.

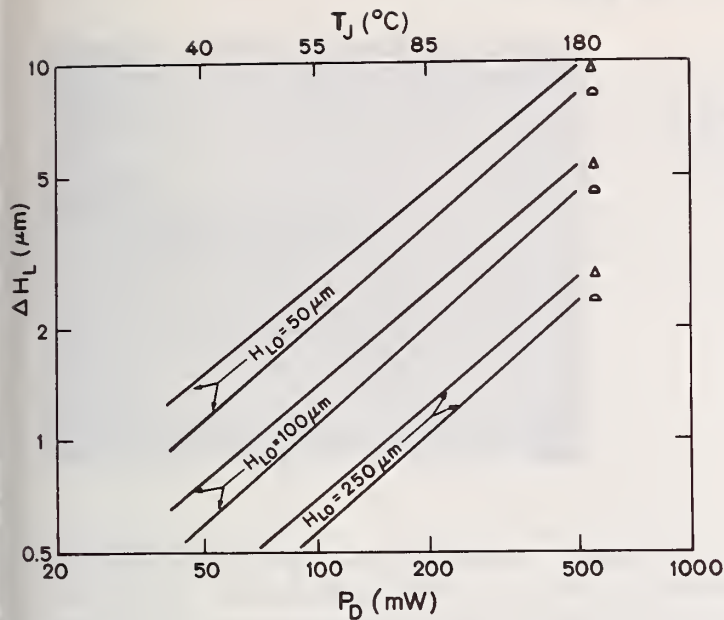


Figure 8. Wire-bond flexure (ΔH_L) as a function of power dissipation (P_D) for triangular (Δ) and semicircular (Δ) loops with several values of initial height (H_{LO}).

If the wire loop is in the form of a triangle, the loop height is given by:

$$H_L = 2[s(s-a)(s-b)(s-L)]^{1/2}/L,$$

where $a + b = S$ and $s = (a + b + L)/2$. This formulation allows the difference in expansion of the die and post ends of the wire, which results from the temperature distribution along the wire, to be taken into account. Results for the case where $a_0 = b_0 = S_0/2$ are identified by triangular symbols in figure 8.

From these plots, it can be seen that regardless of the details of the model the flexure is approximately proportional to power dissipated and approximately inversely proportional to initial loop height. Increasing loop height would be expected to reduce failures from this cause. A group of transistors fabricated with a loop height of 300 to 375 μm survived more than 70,000 slow thermal cycles without a failure whereas in earlier groups failures began to occur from a few hundred to a few thousand cycles. (W. E. Phillips)

Ribbon-Wire Bonding — Problems encountered in setting up the ribbon wire bonding machine were discussed last quarter (NBS Tech. Note 702, p. 19). The most serious problem was a jumping and bouncing motion of the bonding tool immediately after the first bond is made. Although complete correction of this undesired motion can be accomplished only by re-designing the transducer-motion cam, considerable reduction of the undesired motion was achieved by regrinding the appropriate surfaces of the existing cam by hand.

Figure 9. SEM photomicrograph of a rectangular wire-feed hole in an ultrasonic bonding tool. (There is a slight build up of aluminum in the upper left corner of the hole. Magnification: about 750 X.)



The variability of bond tail-length, observed last quarter, was reduced by a factor of two by improving the wire feed mechanism. This tail-length variation, which is only of cosmetic concern to bonding on a laboratory basis, must be controlled before the machine can be used in production since long wire tails may cause short circuits. The remaining tail-length variation now appears to result entirely from the non-uniform dimensions of the available ribbon wire also observed last quarter. This non-uniformity prevents the machine wire cut-off characteristics from being further optimized for a specific wire thickness. For the conditions used, a flatter wire has a shorter tail; a more nearly square wire has a longer tail.

As yet a solution to the control of wire size has not been reached. Contact has been made with several manufacturers. A contract has been let to one supplier to furnish aluminum wire in a variety of sizes and in two different alloys (1 percent silicon or 1 percent magnesium) so that optimum sizes and alloy can be selected.

For bonding with ribbon-wire, the wire feed and clamp mechanism must be modified so that the clamps are horizontal instead of vertical, as is normal with round-wire bonding machines. Two bonding machine manufacturers have developed wire feed and clamp mechanisms; a third has a mechanism under development. Ribbon-wire bonding feasibility, from an economic point of view, would be enhanced if suitable retrofit ribbon-wire clamping mechanisms are made available. Then device manufacturers would not have to invest in new bonders in order to bond devices with ribbon-wire.

Some modification of bonding tools may also be desirable for use in ribbon-wire bonding. At present, a variety of shapes for the bonding face are being studied. Since some of the shapes to be studied are not commercially available, it has been necessary to develop techniques for regrinding tools to the desired shape. The technique for repolishing flat tools (NBS Tech. Note 702, p. 20) is being used to obtain flat surfaces

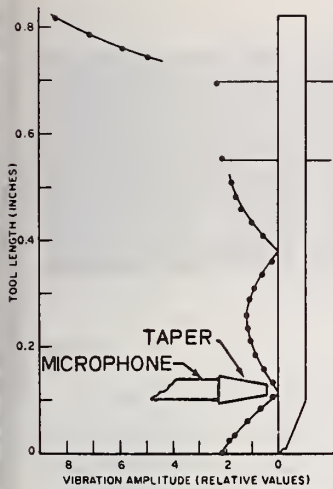


Figure 10. Most desirable placement position for capacitor microphone used in study of variations in vibration amplitudes of the bonding tool at the fundamental driving frequency and its harmonics during bonding. (Measurements may also be made at the upper node, but with somewhat different results.)

which are then modified to a convex or concave shape with or without grooves.

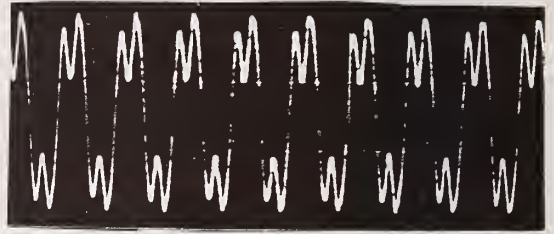
A second modification to the bonding tool that is desirable but not essential is the introduction of a rectangular wire-feed hole. The tools now being used in the experimental work were obtained commercially. An SEM photomicrograph of the rectangular feed hole in one of these tools is shown in figure 9. A different manufacturer has agreed to make such tools if NBS supplies the tungsten ribbon-wire required in the electrical-discharge-machining operation. Although a commercial source of small size tungsten ribbon-wire could not be located, it was a relatively simple process to flatten 0.001-in (25- μm) and 0.002-in. (50- μm) diameter round wire by placing the tungsten wire in a press between glass plates, and applying a load of 6.5 to 11 ksi (45 to 76 MN/m^2) for 0.001-in (25- μm) diameter wire, or 15 to 21 ksi (103 to 145 MN/m^2), for 0.002-in (50- μm) diameter wire, to flatten it. The resulting ribbon was not generally uniform, but pieces could be selected for the desired sizes of rectangular holes.

(H. K. Kessler and G. G. Harman)

In-Process Bond Quality Determination — Work was resumed on the study of bonding tool motion during bonding (NBS Tech. Notes 592, pp. 39-41, and 598, p. 27). The object of this study is to analyze the ultrasonic vibration amplitudes at various points along the bonding tool during the process of making a bond. The detector used in this study is a capacitor microphone that responds to frequencies up to approximately 200 kHz. Information gained from this study is expected to increase the understanding of the ultrasonic bonding process and may lead to an in-process control technique for evaluation of bonds.

Present studies have indicated that the most sensitive and desirable microphone pickup point is at a node of the fundamental frequency on the

Figure 11. A relatively stable waveshape observed 5 to 10 ms after the start of bonding showing individual differences in the harmonic content from peak to peak. (This was obtained with the microphone placed at a node as shown in figure 10. Vertical axis: 20 millivolts per division. Horizontal axis: 20 microseconds per division.)



tool as shown in figure 10. This position has the advantage that the 60-kHz fundamental is essentially cancelled out. Since higher harmonics do not share a common node with the fundamental, their relative amplitude is enhanced. For this application, a hole in the microphone taper (NBS Tech. Note 520, pp. 63-66) of approximately 0.020-in. (0.5-mm) diameter is most suitable since it straddles the node. Under loaded conditions when the tool is transmitting ultrasonic energy into the bond, the node associated with the fundamental shifts by as much as 0.007 in. (0.18 mm) (NBS Tech. Note 520, p. 39). As a result the amplitude of the fundamental increases by about a factor of two, but the amplitudes of various harmonics increase even more.

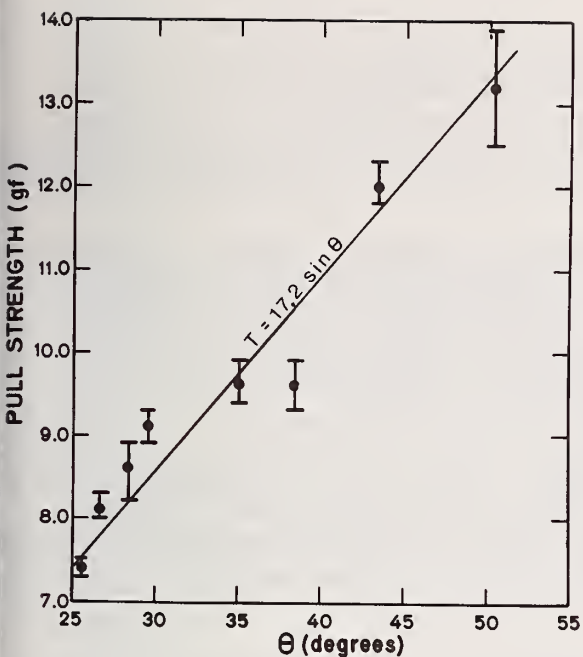
A typical ultrasonic bond with 0.001-in. (25- μ m) diameter aluminum wire is made within 3000 to 6000 cycles of the vibrating bonding tool (50 to 100 ms). The continually changing amplitude, measured at the node, can be described as follows: During the first 10 to 20 cycles the amplitude is small and erratically distorted; the wave shape is primarily the 60-kHz fundamental. Little or no ultrasonic energy appears to be being transmitted into the wire or bonding pad. The amplitude grows rapidly for the next 10 to 20 cycles; the wave shape remains essentially 60-kHz. After 300 to 600 cycles (5 to 10 ms) the amplitude becomes relatively stable; higher harmonics are clearly evident in the waveshape as shown in figure 11. During the next 30 to 40 ms as the bond is made the amplitude increases slowly and the leading peak becomes more prominent.

(G. G. Harman)

Pull Test Evaluation — Work on evaluation of the destructive, double-bond, pull test was resumed. An extensive series of experiments has been initiated to test the effects on the measured pull strength of single-level bond pairs of variation in pull rate, pull angle, and position of the hook along the loop.

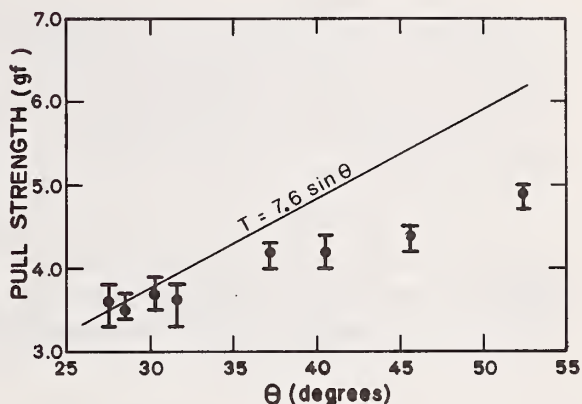
A second series of tests was conducted to determine the effect of variations in bond angle (or ratio of loop height to bond-to-bond spacing) on the measured pull strength of single-level bond pairs pulled at the center of the loop in a direction perpendicular to the plane of the pads. Eight groups of 20 single-level bond pairs were made with different loop

WIRE BOND EVALUATION



a. Unannealed.

Figure 12. Measured pull strength as a function of bond angle (θ). (The solid line is calculated from the resolution of forces; the numerical factor is twice the breaking force in the wire.)



b. Annealed.

heights and spacings. The bond angle varied from 25.7 to 50.3 deg. Ten of the bond pairs in each group were pulled in the unannealed condition; all broke at the heel of the first bond. The remaining groups of 10 were annealed at 500°C for 20 min and then pulled; essentially all broke in the wire span.

Results of the experiment are shown in figure 12. The mean measured pull strength and 95 percent confidence intervals for the mean are plotted for each group against the bond angle; bond angles for the annealed wire have been adjusted to account for the elongation of about 8 percent that occurred before breakage (NBS Tech. Note 592, p. 36). The solid curves are calculated from the resolution-of-forces equation (NBS Tech. Note 555, pp. 31-35) for the symmetrical case under study:

$$T = 2T_w \sin \theta,$$

where T is the measured pull strength, T_w is the force in the wire, and θ is the bond angle. In the unannealed case, where the break occurs at the heel of the first bond, the calculated pull strength agrees with the measured value, but for annealed bonds, where the break occurs in the wire span, the measured pull strength is much less dependent on bond angle. These results are not in agreement with earlier experiments (NBS Tech. Notes 571, pp. 24-26, and 592, pp. 36-37); the origin of the differences has not yet been established. (K. O. Leedy and C. A. Main)

Bibliography and Critical Review — Preparation of an annotated bibliography of limited distribution reports concerned with degradation and testing of wire bonds was begun. The bibliography of the open literature [1] was prepared for printing. Work on the final draft of the critical survey paper continued, and editorial procedures for publication clearance were initiated. (H. A. Schafft)

Plans: Evaluation of ribbon wire for ultrasonic bonding will continue. Further theoretical and experimental work on electronic mixing of bonding tool ultrasonic signals with local oscillators will continue in the effort to better understand and control bonding. Experimental and statistical analysis of significant factors in the wire bond pull test will continue.

The preparation of the bibliography of the open literature will be completed and sent to the printer. The critical survey paper will be prepared for publication clearance. A draft of the bibliography of limited distribution reports will be prepared.

4.3. REFERENCES

4.1. Die Attachment Evaluation

1. Edwards, A. L., TRUMP: A Computer Program for Transient and Steady-State Temperature Distributions in Multidimensional Systems, Lawrence Radiation Laboratory, Univ. of California, Livermore, California, UCRL-14754 Rev. I., 1 May 1968. Available from the National Technical Information Service, Springfield, Virginia 22151.

4.2. Wire Bond Evaluation

1. Schafft, H. A., Wire Bond Electrical Connections- Testing, Fabrication and Degradation- A Bibliography 1957-1971, NBS Tech. Note 593, January, 1972.

5. METHODS OF MEASUREMENT FOR SEMICONDUCTOR DEVICES

5.1. THERMAL PROPERTIES OF DEVICES

Objective: To evaluate and, if necessary, improve electrical measurement techniques for determining the thermal characteristics of semiconductor devices.

Progress: The preliminary round robin on thermal resistance being conducted in cooperation with JEDEC Committee JC-25 on Power Transistors was continued. The 14 test specimens are being measured under specified device operating conditions with thermal resistance test equipment that exists in each participating organization. The temperature sensitive parameter is to be measured 10, 20, 50, and 100 μ s after the termination of the heating power pulse. The devices are now in the hands of the third participant.

The literature search and work on the bibliography on thermal resistance and transient thermal response measurements were resumed.

(F. F. Oettinger)

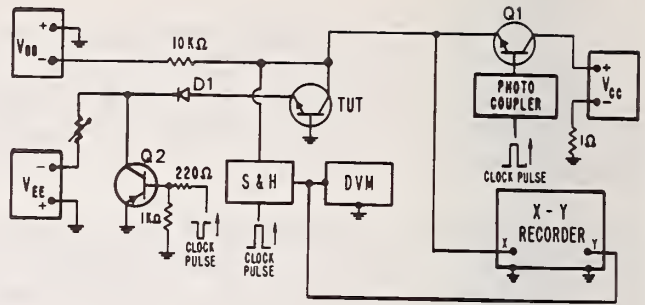
The study was continued to compare other frequently used thermal resistance measuring methods with the common-emitter base-and-collector switching technique. In this technique the base-emitter voltage, V_{BE} , is used as the temperature sensitive parameter, TSP. The common-base thermal resistance measuring circuit in which the emitter-base voltage, V_{EB} , is used as the TSP was modified so that the collector-base voltage could also be used as the TSP. This circuit, shown in figure 13, is generated from the earlier circuit (NBS Tech. Note 702, pp. 23-24) by disconnecting both the sample-and-hold unit and the negative lead of the V_{BB} measuring current supply from the emitter terminal of the transistor under test and reconnecting them to the collector terminal. The new circuit functions in the same manner as the previously described unmodified circuit. In order to facilitate the comparison of the three techniques for measuring thermal resistance a single test unit which incorporates as much common circuitry as possible was fabricated.

Initial measurements made on a triple-diffused power transistor indicated that the difference in thermal resistance when measured using V_{CB} and V_{BE} as the TSP was less than 10 percent of the average value, while for measurements made on a wide-base, single-diffused power transistor the difference was less than 5 percent. In both cases, using V_{CB} as the TSP gave lower values of thermal resistance than using V_{BE} . It is not yet apparent whether this difference is real or due in part to effects of non-thermal switching transients.

At one time during the quarter it was found that the difference between thermal resistance as measured by the V_{EB} and V_{BE} methods increased from the 2 or 3 percent reported previously (NBS Tech. Note 702, pp. 25-26) to approximately 10 percent. The cause of this deviation was traced

THERMAL PROPERTIES OF DEVICES

Figure 13. Common-base circuit for measuring thermal resistance of transistors using the collector-base voltage as the temperature sensitive parameter.



to excessive leakage through the biased-off collector switching transistor, Q1. This observation showed the importance of using a very low-leakage device in this position in the measuring circuit.

(S. Rubin and F. F. Oettinger)

Plans: The literature search and work on the bibliography on thermal resistance and transient thermal response measurements will continue. The comparison of thermal resistance measurements using V_{BE} , V_{EB} , and V_{CB} as temperature sensitive parameters will continue; measurements will be made on a variety of device types.

5.2. THERMOGRAPHIC MEASUREMENTS

Objective: To evaluate the utility of thermographic techniques for the detection of hot spots and measurement of temperature distribution in semiconductor devices.

Progress: Initial attempts were made to coat various devices with phosphors by the slurry-settling technique (NBS Tech. Note 702, p. 28). It does not appear possible at this time to coat each device with an opaque, uniform, and controlled thickness of phosphor because of difficulties associated with the device surface contour, header construction, device position on the header, lead size, and lead location. As a result, it is not possible to eliminate the necessity of calibrating each point on a phosphor-coated device at which it is desired to know the temperature. The calibration is accomplished by maintaining the device in an unpowered state at a known temperature and measuring the fluorescent intensity of the phosphor at each point of interest for a constant intensity of ultraviolet radiation. The temperature of the device during calibration is varied to span the entire expected temperature range of the surface when the device is operated.

Further studies were made of both microcopy resolution charts (NBS Tech. Note 592, p. 56) and metallization patterns on silicon and silicon dioxide to determine their suitability for measuring the spatial resolution

of the 50- μm fiber-optic probe. Neither had a sharp enough transition from the white, highly reflecting to the black, poorly reflecting surfaces to be suitable for this purpose. The information to date indicates that the distance over which the apparent intensity as measured with the fiber optic probe varies from 10 to 90 percent of the total intensity change at a step boundary is no more than 35 μm .

Measurements were made to compare the relative uniformity of phosphor coatings deposited by the slurry-settling technique and the water-flotation technique. The 50- μm fiber-optic probe was scanned over a 1-mm long region of the coated wafer. The scans were made on a wafer coated with a phosphor with a temperature sensitive range of 120 to 280°C for six different temperatures within the temperature range. For each of the temperatures, the standard deviation about the average phosphor intensity for the water-flotation technique was about ± 10 percent (approximately equal to $\pm 2^\circ\text{C}$) and for the slurry settling technique about ± 3 percent ($\pm 0.6^\circ\text{C}$). The difference is a result of the thicker coating one can obtain using the slurry-settling technique (about 50 μm in this instance) compared to the water-flotation technique (generally about 10-15 μm thick).

Preliminary experiments have been performed to establish if it is feasible to use the photomultiplier tube and present optical equipment to measure the transient response of the phosphors to a heat pulse. The measurements were performed on a transistor chip coated with a phosphor that covers the range from room temperature to 80°C. It was found that noise on the output of the photomultiplier tube was great enough that quantitative measurements would be very difficult without cooling the tube. Recent work by Blanks [1] indicates that the best response time one can achieve with the phosphors of the type being used is 200 μs . This is hardly fast enough to be of much value as a transient thermographic technique for device studies. Blanks [1] does mention a phosphor with a response time of 35 μs , but the thermal sensitivity (2 percent change in intensity per degree Celsius) is probably too small to make it of use as a thermographic tool.

A survey of the literature concerned with thermographic techniques other than thermographic phosphors is being conducted. The technique which is now of greatest value for thermographic device studies is infrared microscopy. Scanning electron microscopy and holographic microscopic interferometry are two other methods which are of potential value for thermographic device studies. (D. L. Blackburn and L. R. Williams)

Plans: To conclude the evaluation phase of the thermographic phosphor study, experiments will be designed to determine the spatial-temperature resolution of the phosphors and to establish the accuracy with which the temperature of a hot spot can be measured with the phosphors. These experiments will require an independent measurement of the temperature distribution of the devices under study. An infrared microradiometer will be obtained for this independent measurement; experimental work will not begin until April, 1972.

5.3. MICROWAVE DEVICE MEASUREMENTS

Objective: To study the problems and uncertainties associated with the measurement of microwave devices, and to improve the techniques of these measurements.

Progress: Lack of rigidity in the waveguide system has been reported as a limitation on the precision that can be achieved in making conversion loss measurements (NBS Tech. Note 702, p. 30). To obtain detailed reproducibility data on the original waveguide system, the supporting jacks were adjusted to give the most stable and uniform support, and 16 type 1N23 (and equivalent) diodes of assorted makes and suffix letters (mostly WE's, with some E's and D's) were measured for insertion loss (conversion loss without i.f. mismatch correction) using the incremental modulation method described last quarter (NBS Tech. Note 702, pp. 29-30). Each diode was measured twice after insertion in the holder; it was then removed from the holder and immediately reinserted with the same angular orientation and again measured twice before removal. An identical run was made the following day, after the local oscillator power had been re-adjusted with a bolometer substituted for the mixer. Two diodes appeared to be unstable, as evidenced by large loss differences. Excluding these unstable devices it was found that differences between pairs of readings taken on the same diode after removal and reinsertion were, on the average, about twice as large as differences between pairs of readings taken at the same time without removing the diode between readings. It was also found that, excluding the two unstable devices, differences between pairs of readings from the two runs conducted on successive days were on the average about three times as large as differences between pairs of readings taken at the same time without removing the diode between readings. It has not yet been determined how much of this additional variation was due to waveguide motion, how much to lack of reproducibility at the diode contact and waveguide flange, and how much to local oscillator and voltmeter drift.

To prevent power changes due to waveguide motion, a clamping-type support system has been designed and constructed. The support system consists of the following: A lower base plate of $\frac{1}{4}$ -in. thick aluminum alloy covering the bench top supports an upper base plate of the same size and material. The upper base plate is divided into two sections, one of which supports that part of the waveguide structure that will be sent to NBS-Boulder for noise calibration. The upper base plate sections were drilled and tapped at 1-in. intervals over their surfaces to accept threaded brass rods used in clamping the waveguide. The threaded rods pass through aluminum alloy waveguide support blocks to which they are rigidly locked by nuts. The waveguide is held down against each support block by an aluminum alloy top plate which is drilled to clear the rods and secured with even pressure by means of wing nuts.

In order to facilitate clamping of the waveguide to the base plate, and to accommodate the lesser but more critical power requirements of a new type of synchronizer used to phase-lock the klystron, the waveguide

MICROWAVE DEVICE MEASUREMENTS

system between the klystron and the modulation attenuator was rebuilt. Most of the changes were mechanical, to eliminate elevation of some components over other components. Minor electrical changes include the substitution of a 20 dB directional coupler to connect the leveling loop detector for the 10 dB coupler previously used (NBS Tech. Note 598, pp. 36-38), the addition of a level-set attenuator next to the phase-lock (synchronizer) coupling in order to reduce the power to an optimum level, and the return to the use of a hybrid tee (NBS Tech. Note 560, p. 43) in place of the 20 dB directional coupler used to divide power between the phase-lock (synchronizer) and the wavemeter. The resulting power increase to the wavemeter allows the making of klystron adjustments with a passive D'Arsonval-Weston type microammeter instead of with the more sluggish and less stable electronic galvanometer.

The rotary-vane type precision attenuator, used to set the power incremental in the incremental modulation method of measuring mixer conversion loss, was modified by the addition of two lockable 0- to 1-in. vernier micrometer heads that engage round-headed fixed stops screwed to opposite assembly flanges of the rotating drum holding the center vane. In order to use this attenuator to set precisely two independent power increments (one above and the other below the local oscillator level) an attempt is currently being made to add a third stop to be used to establish the upper increment, from local oscillator level to modulation peak. The micrometer head for this stop is mounted on a hinged platform so that it may be swung clear to allow use of the other stop on the same side of the rotating drum. This second stop is used to establish the more critical and more frequently required peak-to-trough bilateral increment. Both of these increments also depend upon the stop on the opposite side of the rotating drum. By keeping this stop at the zero vane angle position its uncertainty contribution is minimized. These modifications not only greatly increase the accuracy that can be achieved, but allow the attenuator to be used directly as the modulator, instead of using it to calibrate the electrical (leveling loop) modulator, should the latter prove to be insufficiently repeatable.

Visits were made to two major suppliers of microwave mixer diodes in order to discuss measurement requirements for these devices and to obtain information and guidance for the planning of future activities in this area. These discussions indicated that the fixed-tuned MIL-standard holders (diode mounts) for the various frequency bands may not be sufficiently reproducible, although there was disagreement between manufacturers as to which bands presented the most serious problems. It appears that the holder problem may have to be studied at an earlier phase in the program than had been anticipated.

(J. M. Kenney)

Plans: The first meeting of the IEEE Task Group concerned with mixer diodes and video detector diodes will be held at NBS early next quarter. This group is a part of the IEEE-GED Standards Committee for Electron Devices. The main item to be discussed at this meeting is IEC document

47(Central Office)376. The subject of this document is general principles of measuring methods for mixer diodes used at microwave frequencies.

Fabrication of the third attenuator stop and installation of the clamping-type waveguide support system will be completed. Additional conversion loss measurements will be taken to estimate the repeatability that can be achieved with the modified system. The precision modulation attenuator and the bolometers used for power measurement will be calibrated at NBS-Boulder.

5.4. CARRIER TRANSPORT IN JUNCTION DEVICES

Objective: To improve methods of measurement for charge carrier transport and related properties of junction semiconductor devices.

Progress: Preliminary intercomparison measurements of transistor delay time have been made on the Sandia bridge [1] and vector voltmeter. Under some conditions of measurement, significantly different values were obtained for this characteristic that is frequently used as a screen in radiation hardness assurance tests. Both S-parameter systems have been assembled and familiarization tests begun. Additional study has been completed on the problem of high-frequency electrical probing of semiconductor devices at the wafer stage. An analysis was completed which relates delay time as measured by the Sandia bridge and the vector voltmeter to internal device time constants.

Experimental - Intercomparison measurements of transistor delay time have been started on the two completed measurement systems. In describing the initial results, one of these systems is designated as system A and the other as system B. Measurements were made on three transistor types: 2N2219, 2N2222, and 2N2907A. These are all low power (less than one watt) silicon units. The first two types are *n-p-n* and the last is a *p-n-p*. Measurements of delay time were made on each system for various frequencies between 3 and 30 MHz and at various emitter currents up to about 50 mA. The collector-base junction had a constant reverse bias of 5 V. In some cases, the transistors oscillated initially, but this was cured by threading ferrite beads onto the collector leads.

For a given transistor and measurement frequency, the measured delay time decreased with emitter current in the manner expected, and asymptotically reached its minimum value at a current between 30 and 50 mA, for both systems. For 2N2219 transistors, as measured with system A, the shapes of the curves of delay-time as a function of emitter current were similar; for frequencies between about 3 and 10 MHz, the curves were displaced significantly one from the other, but for measurements made between 10 and 30 MHz the curves were within about 5 percent of one another. For all devices, system A consistently produced larger delay-time readings than system B. Typically, as compared with system B under the same conditions of measurement frequency, transistor, and bias condition, system

A yielded an asymptotic value of delay time that was higher for a 2N2219 by 29 percent; for a 2N2222, by 37 percent; and for a 2N2907, by 17 percent. (F. R. Kelly and D. E. Sawyer)

The components for the two S-parameter measurement systems were received, checked for performance, and assembled. Devices were measured to check the performance of these systems and to familiarize personnel with their operation. (G. J. Rogers)

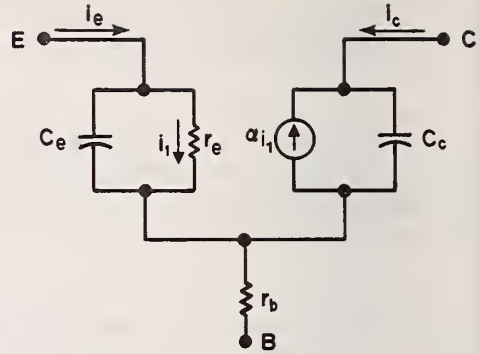
Probing Studies - Additional study was conducted of the problem of electrical probing of semiconductor devices while they are at the wafer stage of preparation. This study, based both on a survey of the literature and past experiences, included consideration of various instruments available to make probe-type measurements at frequencies up to a few gigahertz, of both reversible and non-reversible effects of probe pressure on device parameters, and of the influence of contact resistance and stray capacitances on the measurements. An informal letter report that summarizes the results of this investigation is being prepared for the sponsor. (D. E. Sawyer)

Analytical - The analysis relating delay time as measured by the Sandia bridge and vector voltmeter circuit to the various time constants and delay times within the device has been completed. These measurement circuits have the common characteristic that the a-c signal voltage between the transistor collector and base terminals is zero when the delay time is measured. This is accomplished in the Sandia bridge with the use of a "bucking" or "nulling" signal from a phase-splitter and electrical delay circuit and, more simply, in the vector voltmeter setup by bypassing the transistor collector to the base (ground). Because of this common operating characteristic, it is appropriate that both be analyzed in the same way; it turns out that the resulting expressions for measured delay time are generically similar. Although this analysis is based on simplified models for the measuring circuits, the methodology employed may be extended to other, more complex, models or circuits.

A surprising result of this analysis is that neither circuit measures the sum of the propagation delays between the emitter and collector leads, as one might expect. On the contrary, certain time constants may diminish the delay time measured. This is because the measurement yields the phase, rather than the group delay time. The phase delay is the delay of the carrier frequency, ω , while the group delay represents the delay of the envelope of the input signal or the propagation delay of the information contained in the input signal. The quantity measured, the phase delay, may differ from the (true) propagation delay if certain RC time constants exist.

The analysis, which is reported in greater detail elsewhere [2], is based on the widely used transistor model shown in figure 14. This equivalent circuit is expected to represent mesa devices quite well. This

Figure 14. Equivalent circuit used to model a transistor for analysis of delay-time measurements.



circuit is perhaps the simplest transistor representation for the analysis of delay-time measurements. Other types of transistors might require the addition of other passive elements, such as an additional capacitor between the top of the current generator and "B", the base terminal, to represent the base-collector overlap diode capacitance of a planar transistor or a resistor in series with "C", the collector terminal, to represent the collector series resistance.

In figure 14, C_e and C_c are the transition-region capacitances of the emitter-base and base-collector junctions, respectively, r_b represents the base resistance, and r_e represents the dynamic resistance of the (forward-biased) emitter junction. For forward emitter currents much larger than the emitter-base diode saturation current,

$$r_e = kT/qI_E, \tag{1}$$

where k is Boltzmann's constant, T the absolute temperature, q the electronic charge, and I_E the dc emitter current. At room temperature, $r_e = 26/I_E$ ohms if I_E is given in milliamperes. Only i_1 , the current through r_e , is effective in producing transistor action. The current source in the collector circuit represents the active portion of the transistor operation and is specified as the product of i_1 and α , the small-signal base-transport coefficient. In general, α is complex and varies with frequency. It can always be written $\alpha = |\alpha(\omega)| \exp(-j\omega\tau_\alpha)$, where $|\alpha(\omega)|$ is an even function of frequency and τ_α is the delay time associated with the transit of minority carriers across the base region and across the collector junction. The quantity τ_α may itself be a function of frequency. It is convenient to define the time constants $\tau_e \equiv r_e C_e$ and $\tau_c \equiv r_b C_c$. From eq (1) it is clear that τ_e varies inversely with emitter current and that it can be made negligibly small if sufficiently large emitter currents are used.

In the vector voltmeter circuit the quantity read is the phase shift

between the transistor emitter and collector currents. The emitter-collector phase delay time, τ , in seconds, is related to the measured phase shift by

$$\tau = \theta/\omega,$$

where θ is the phase angle in radians and ω is the signal angular frequency.* If, as is usually the case, $\omega\tau \ll 1$, then τ , is related to the delay times defined above by

$$\tau = \tau_{\alpha} + \tau_e - \tau_c/h_{fe}, \quad (2)$$

where h_{fe} is the small-signal common-emitter current gain (as usually defined).^{fe} Note that h_{fe} , rather than h_{fb} , appears in eq (2), even though the transistor base is the common element in the measurement circuit.

Equation (2) states that the delay time, as determined from the measured emitter-collector current phase angle, is the sum of τ_{α} and τ_e diminished by the collector-base RC time constant divided by the common-emitter current-gain. For most good-quality transistors, h_{fe} is sufficiently large, and τ_c sufficiently small, so that this τ_c/h_{fe} term may be neglected, and so the delay time measured will be simply the sum of τ_{α} and τ_e . However, following irradiation, h_{fe} is expected to drop and τ_c to increase (as a result of an increase in r_b). Then it is possible that the τ_c/h_{fe} term may affect the delay time measured.

To analyze the idealized Sandia bridge, it is necessary to include in the equivalent circuit an impedance, R_z , in series with both the emitter and collector of the transistor. This impedance is the sum of the load and source impedances for the delay lines. In the present case R_z is 100 Ω , twice the characteristic impedance of the delay lines. With these additions and the assumption that $\omega\tau \ll 1$, the measured delay time is given by

*

For θ in degrees and the frequency, f , in hertz, the expression for τ in seconds is

$$\tau = \theta / (360 f).$$

A particularly useful form of this equation expresses the delay time in nanoseconds in terms of the frequency in megahertz and the phase angle in degrees:

$$\tau_{(ns)} = (2.78/f_{MHz}) \text{ per degree.}$$

A one degree phase shift at 27.8 MHz would indicate a delay time of 0.1 ns, for example.

$$\tau = \left(\frac{1}{1 - \frac{|\alpha(\omega)| r_b}{R_z + r_e + r_b}} \right) \left\{ \tau_\alpha + \left(1 - \frac{r_e}{R_z + r_e + r_b} \right) \tau_e - \left(\frac{\tau_c}{h_{fe}} \right) \right\} \quad (3)$$

Note that if $R_z \rightarrow \infty$, then this delay time expression for the idealized Sandia bridge becomes identical with eq (2), the delay time expression for the vector voltmeter. The quantities r_e , r_b , and $|\alpha(\omega)|$ can all be determined and so the correction factors multiplying the delay time components—the factors in the parentheses—can be computed. The same general comments about the term τ_c/h_{fe} made above in connection with the vector voltmeter also apply.

Another result of this analysis is the finding that the delay time of RC elements suitably combined on transistor headers can be calculated. Thus, they can be expected to provide a means to check the overall operation of delay-time instruments and make a convenient means to spot-check their calibration. (D. E. Sawyer)

Plans: Passive networks will be made for making comparison measurements on the several measurement systems. The results of the S-parameter measurements will be related to the physics of the devices under test. Now that the required accessories have been received the vector voltmeter will be calibrated against passive networks. Transistor intercomparison delay-time measurements will be continued; attempts will be made to resolve the differences between systems.

5.5. SILICON NUCLEAR RADIATION DETECTORS

Objective: To conduct a program of research, development, and device evaluation in the field of silicon nuclear radiation detectors with emphasis on the improvement of detector technology, and to provide consultation and specialized device fabrication services to the sponsor.

Progress: Study of 2-MeV proton radiation damage effects in lithium-drifted silicon detectors has been completed. Ambient exposure tests were delayed because of the appearance of anomalous effects.

Radiation Damage — The experimental portion of the study of proton radiation damage effects has been completed with the irradiation of two, 2-mm thick, lithium-drifted silicon detectors by protons of approximately 2-MeV energy. Both detectors were reverse biased at 400 V during the irradiation which was carried out at room temperature; one detector was irradiated through the front (*p*-contact) and the other through the rear (*n*-contact).

For the detector irradiated through the *p*-contact, a rapid increase of leakage current and noise was observed with increased proton fluence above $3 \times 10^{11} \text{ cm}^{-2}$. After irradiation at a fluence of $2 \times 10^{12} \text{ cm}^{-2}$, the leakage current was 3.5 μA , measured at room temperature, and the noise was 80 keV, compared with 1.5 μA and 15 keV, respectively, before irradiation. A dead layer was observed at the irradiated contact, but the detector exhibited little change in capacitance throughout the irradiation. Protons of the energy used have a range of approximately 45 μm in silicon and thus introduce defects into a volume small relative to the total space charge region.

The degradation of detector performance observed for the device irradiated through the *n*-contact occurred at a much lower rate than that for the front-contact irradiation. No change in charge collection efficiency was observed at fluences up to approximately 10^{14} cm^{-2} . The fabrication process for lithium-drifted detectors results in a dead region at the *n*-contact. This detector had a dead layer of about 50 μm ; therefore, proton-induced defects would be localized mainly in the *n*-contact outside the sensitive depletion region. The only significant changes that were observed were increases in contact noise (from 17 to 17 to 27 keV) and leakage current (from 1.5 to 2.3 μA) after irradiation at a fluence up to 10^{14} cm^{-2} .

Both detectors exhibited annealing effects in leakage current and detector noise when they were kept under reverse bias of 400 V at room temperature. For the detector irradiated through the *p*-contact, the current decreased to 2 μA and the noise to 35 keV after 3 days. For the other detector, the current decreased almost to its pre-irradiation level after 1 day, and the noise decreased to 20 keV after 2 days.

Measurements were begun using the infrared response technique on lithium-drifted silicon detectors which had been irradiated with neutrons or electrons (see Section 3.3). (Y. M. Liu)

Ambient Exposure Tests - Anomalous effects observed during the operation of the test chamber did not permit dry ammonia measurements to be concluded on three silicon surface barrier detectors. The origin of these effects, whether due to contamination in the vacuum system or behavior of this type of detector at low pressures, is not understood at the present time. (W. K. Croll)

Plans: Further neutron irradiation will be performed to gain additional information on the long-term stability of lithium-drifted and surface-barrier silicon nuclear radiation detectors. Results obtained thus far in the study of nuclear radiation damage effects in lithium-drifted silicon detectors will be analyzed in preparation for possible publication. Measurements of infrared response on lithium-drifted silicon detectors, before and after neutron irradiation will continue. The study of the effects on detector performance of dry ammonia and hydrogen,

SILICON NUCLEAR RADIATION DETECTORS

the main reaction products of the hydrazine used in spacecraft thrusters, will continue once the source of the anomalous observations has been ascertained and corrected.

5.6. REFERENCES

5.2. Thermographic Measurements

1. Blanks, H. S., The Transient Behaviour of ZnS-Type Phosphors used in Thermography, *Proc. I.R.E.E. (Aust)* 31, 397-405 (1970).

5.4. Carrier Transport in Junction Devices

1. Sullivan, W. H., A New Technique for the Direct Measurement of Minority Carrier Base Transit Time in the Junction Transistor, Sandia Laboratories Report SC-DR-69-419, September, 1969. Available from the National Technical Information Service, Springfield, Va. 22151
2. Sawyer, D. E., A Simple Analysis of Idealized Delay-Time Measurement Circuits, NBS Technical Note (in preparation).

Appendix A

JOINT PROGRAM STAFF

Coordinator: J. C. French
Consultant: C. P. Marsden

Semiconductor Characterization Section
(301) 921-3625

Dr. W. M. Bullis, Chief

F. H. Brewer
M. Cosman
Dr. J. R. Ehrstein
R. L. Mattis

Dr. W. E. Phillips
Miss D. R. Ricks
H. A. Schafft

Miss K. E. Smith⁺
A. W. Stallings
Mrs. M. L. Stream⁺
W. R. Thurber

Semiconductor Processing Section
(301) 921-3541

Dr. A. H. Sher, Acting Chief^x

H. A. Briscoe
W. K. Croll
Mrs. S. A. Davis⁺
H. E. Dyson*
G. G. Harman

W. J. Keery
H. K. Kessler
J. Krawczyk
T. F. Leedy

Y. M. Liu
Mrs. J. M. Guyton
Mrs. E. A. Simmons[¶]
L. M. Smith
G. P. Spurlock

Electron Devices Section
(301) 921-3622

J. C. French, Chief

D. L. Blackburn
Mrs. C. F. Bolton⁺
Miss B. S. Hope⁺
R. L. Gladhill
F. R. Kelly[¶]

J. M. Kenney
Mrs. K. O. Leedy[§]
Miss C. A. Main[§]
F. F. Oettinger

M. K. Phillips
G. J. Rogers
S. Rubin
D. E. Sawyer
L. R. Williams

* Part Time

+ Secretary

¶ Summer

x Dr. J. A. Coleman is on temporary assignment to Office of Associate
Director for Programs.

§ Telephone: (301) 921-3625

Appendix B

COMMITTEE ACTIVITIES

ASTM Committee F-1 on Electronics

- C. F. Bolton, Committee Assistant Secretary
- W. M. Bullis, Editor, Subcommittee 4, Semiconductor Crystals, and Subcommittee 7, Hybrid Microelectronics; Leaks, Resistivity, Mobility, Dielectrics, and Compound Semiconductors Sections
- J. A. Coleman, Secretary, Subcommittee 5, Semiconductor Processing Materials
- J. R. Ehrstein, Chairman, Resistivity Section, Epitaxial Resistivity, and Epitaxial Thickness Sections
- J. C. French, Committee Editor
- G. G. Harman, Interconnection Bonding Section
- K. O. Leedy, Chairman, Interconnection Bonding Section
- T. F. Leedy, Photoresist Section
- C. P. Marsden, Committee Secretary
- R. L. Mattis, Lifetime Section
- W. E. Phillips, Chairman, Lifetime Section; Secretary, Subcommittee 4, Semiconductor Crystals; Crystal Perfection, Encapsulation, Thin Films, and Thick Films Sections
- A. H. Sher, Germanium Section
- W. R. Thurber, Mobility, Germanium, Compound Semiconductors, and Impurities in Semiconductors Sections

ASTM Committee E-10 on Radioisotopes and Radiation Effects

- W. M. Bullis, Subcommittee 7, Radiation Effects on Electronic Materials
- J. C. French, Subcommittee 7, Radiation Effects on Electronic Materials

Electronic Industries Association: Solid State Products Division, Joint Electron Device Engineering Council (JEDEC)

- J. M. Kenney, Microwave Diode Measurements, Committee JC-21 on UHF and Microwave Diodes
- F. F. Oettinger, Chairman, Task Group JC-11.3-1 on Thermal Considerations for Microelectronic Devices, Committee JC-11 on Mechanical Standardization; Technical Advisor, Thermal Resistance Measurements, Committees JC-22 on Rectifier Diodes and Thyristors, JC-20 on Signal Diodes, JC-25 on Power Transistors, and JC-30 on Hybrid Integrated Circuits
- S. Rubin, Chairman, Council Task Group on Galvanomagnetic Devices
- H. A. Schafft, Technical Advisor, Second Breakdown and Related Specifications, Committee JC-25 on Power Transistors

IEEE Electron Devices Group:

- J. C. French, Standards Committee
- J. M. Kenney, Chairman, Standards Committee Task Force on Microwave Solid-State Devices II (Mixer and Video Detector Diodes)

APPENDIX B

H. A. Schafft, Chairman, Standards Committee Task Force on Second Breakdown Measurement Standards

IEEE Nuclear Science Group:

J. A. Coleman; Administrative Committee; Nuclear Instruments and Detectors Committee; Editorial Board, *Transaction on Nuclear Science*

IEEE Magnetics Group

S. Rubin, Chairman, Galvanomagnetic Standards Subcommittee

IEEE Parts, Hybrids, and Packaging Group

W. M. Bullis, New Technology Subcommittee, Technical Committee on Hybrid Microelectronics

Society of Automotive Engineers

J. C. French, Subcommittee A-2N on Radiation Hardness and Nuclear Survivability

W. M. Bullis, Planning Subcommittee of Committee H on Electronic Materials and Processes

IEC TC47, Semiconductor Devices and Integrated Circuits:

S. Rubin, Technical Expert, Galvanomagnetic Devices; U.S. Specialist for Working Group 5 on Hall Devices and Magnetoresistive Devices

NMAB ad hoc Committee on Materials and Processes for Electron Devices

W. M. Bullis

NMAB ad hoc Committee on Materials for Radiation Detection Devices

D. E. Sawyer

Appendix C

SOLID-STATE TECHNOLOGY & FABRICATION SERVICES

Technical services in areas of competence are provided to other NBS activities and other government agencies as they are requested. Usually these are short-term, specialized services that cannot be obtained through normal commercial channels. Such services provided during the last quarter are listed below and indicate the kinds of technology available to the program.

1. Failure Analysis (W. J. Keery)
Material from an aircraft air conditioning unit was inspected for the Naval Weapons Engineering Support Activity using the scanning electron microscope and x-ray energy analysis for the presence of foreign particles.
2. Radiation Detectors (W. K. Croll)
An ion-implanted silicon nuclear radiation detector was mounted and connections attached so that it could be used at liquid helium temperatures for the Nuclear Spectroscopy Section.
3. Silicon Weight (M. Cosman and W. K. Croll)
A weight to be used in the determination of vacuum pump fluid density was fabricated from a single crystal of silicon for the Pressure and Vacuum Section.
4. Electrical Burnout Studies (H. A. Schafft, K. O. Leedy, and W. J. Keery)
Electrical tests and visual and scanning electron microscope examinations were conducted on 17 devices (transistor pairs and transistors) for the Harry Diamond Laboratories to assist in establishing degradation and failure modes.

Appendix D

JOINT PROGRAM PUBLICATIONS

Prior Reports:

A review of the early work leading to this Program is given in Bullis, W. M., Measurement Methods for the Semiconductor Device Industry—A Review of NBS Activity, NBS Tech. Note 511, December, 1969.

Quarterly reports covering the period since July 1, 1968, have been issued under the title Methods of Measurement for Semiconductor Materials, Process Control, and Devices. These reports may be obtained from the Superintendent of Documents (Catalog Number C.13.46:XXX) where XXX is the appropriate technical note number. Microfiche copies are available from the National Technical Information Service (NTIS), Springfield, Virginia 22151.

Quarter Ending	NBS Tech. Note	Date Issued	NTIS Accession No.
September 30, 1968	472	December, 1968	AD 681330
December 31, 1968	475	February, 1969	AD 683808
March 31, 1969	488	July, 1969	AD 692232
June 30, 1969	495	September, 1969	AD 695820
September 30, 1969	520	March, 1970	AD 702833
December 31, 1969	527	May, 1970	AD 710906
March 31, 1970	555	September, 1970	AD 718534
June 30, 1970	560	November, 1970	AD 719976
September 30, 1970	571	April, 1971	AD 723671
December 31, 1970	592	August, 1971	AD 728611
March 31, 1971	598	October, 1971	AD 732553
June 30, 1971	702	November, 1971	AD 734427

Current Publications:

Brenner, D. J.,* A Technique for Measuring the Surface Temperature of Transistors by Means of Fluorescent Phosphor, NBS Tech. Note 591, July, 1971.

Sher, A. H., and Thurber, W. R., Minority Carrier and Lithium-Ion Drift Mobilities and Oxygen Concentration in p-Type Germanium, *J. Appl. Phys.* 42, 4508-4509 (October, 1971).

Sher, A. H., Croll, W. K., and Thurber, W. R., Determination of Oxygen in Germanium Below 20 Parts per Billion by Measurements of Lithium Mobility and Precipitation, *Anal. Chem.* 43, 1831-1834 (November, 1971).

* NBS Measurement Engineering Division

APPENDIX D

Harman, G. G., Ultrasonic Systems and Mechanisms of Bonding, presented at the Advanced Microelectronics Techniques Conference, Los Angeles, Calif., September 30, 1971.

Sher, A. H., Keery, W. J., and Dyson, H. E., Improved Infrared Response Measurements in Semiconductor Nuclear Radiation Detectors, presented at the 1971 Nuclear Science Symposium, San Francisco, November 5, 1971, *IEEE Trans. Nucl. Sci.* NS-19, No. 1, 341-344 (February, 1972).

Schafft, H. A., Wire-Bond Electrical Connections: Testing, Fabrication, and Degradation, A Bibliography - 1957-1971, NBS Technical Note 593 (January, 1972).

Sher, A. H., and Keery, W. J., Improved Infrared-Response Technique for Determining Impurity and Defect Levels in Semiconductors, *Appl. Phys. Lett.* 20, 120-122 (1 February 1972).

Marsden, C. P., Tabulation of Data on Semiconductor Amplifiers and Oscillators at Microwave Frequencies, NBS Technical Note 597 (December, 1971).

U.S. DEPT. OF COMM. BIBLIOGRAPHIC DATA SHEET	1. PUBLICATION OR REPORT NO. NBS-TN-717	2. Gov't Accession No.	3. Recipient's Accession No.
4. TITLE AND SUBTITLE Methods of Measurement for Semiconductor Materials, Process Control, and Devices. Quarterly Report, July 1 to September 30, 1971.		5. Publication Date April 1972	6. Performing Organization Code
7. AUTHOR(S) W. Murray Bullis, Editor		8. Performing Organization	
9. PERFORMING ORGANIZATION NAME AND ADDRESS NATIONAL BUREAU OF STANDARDS DEPARTMENT OF COMMERCE WASHINGTON, D.C. 20234		10. Project/Task/Work Unit No. See Item 15	11. Contract/Grant No. See Item 12
12. Sponsoring Organization Name and Address NBS, DASA (EA071-801), Navy Strategic Systems Project Office, NAD, Crane, Indiana (PO-2-0023), NAVELEX (PO-2-1034), AFWL (F29601-71-F-0002), AFCRL (Y71-906), ARPA (MIPR FY76167100331), AEC, NASA (S-70003-G).		13. Type of Report & Period Covered Interim July 1 to September 30, 1971	14. Sponsoring Agency Code
15. SUPPLEMENTARY NOTES 4251126, 4252128, 4254115, 4259522, 4259533, 4252534, 4252535, 4251536, 4254422, 4259425, 4254429.			
16. ABSTRACT (A 200-word or less factual summary of most significant information. If document includes a significant bibliography or literature survey, mention it here.) This quarterly progress report, thirteenth of a series, describes NBS activities directed toward the development of methods of measurement for semiconductor materials, process control, and devices. Significant accomplishments during this reporting period include the disclosure of substantial differences in measurements of transistor delay time, a device characteristic frequently used as a screen in radiation hardness assurance tests, as measured with two different instruments; successful application of the infrared response technique to the study of radiation-damaged, lithium-drifted silicon detectors; and identification of a condition that minimizes wire flexure and reduces the failure rate of transistors under slow thermal cycling conditions. Work is continuing on measurement of resistivity of semiconductor crystals; study of gold-doped silicon; specification of germanium for gamma-ray detectors; evaluation of wire bonds and die attachment; measurement of thermal properties of semiconductor devices; noise properties of microwave diodes; and characterization of silicon nuclear radiation detectors. Supplementary data concerning staff, standards committee activities, technical services, and publications are included as appendixes.			
Key Words (cont.): measurement; microelectronics; microwave diodes; nuclear radiation detectors; probe techniques (a-c); resistivity; semiconductor devices; semiconductor materials, semiconductor process control; silicon; thermal resistance; thermographic measurements; ultrasonic bonder; wire bonds.			
17. KEY WORDS (Alphabetical order, separated by semicolons) Alpha-particle detectors; aluminum wire; base transit time; carrier lifetime; die attachment; electrical properties; epitaxial silicon; gamma-ray detectors; germanium; gold-doped silicon; infrared response; methods of			
18. AVAILABILITY STATEMENT <input checked="" type="checkbox"/> UNLIMITED.	19. SECURITY CLASS (THIS REPORT) UNCLASSIFIED	21. NO. OF PAGES 52	
<input type="checkbox"/> FOR OFFICIAL DISTRIBUTION. DO NOT RELEASE TO NTIS.	20. SECURITY CLASS (THIS PAGE) UNCLASSIFIED	22. Price 55¢	



NBS TECHNICAL PUBLICATIONS

PERIODICALS

JOURNAL OF RESEARCH reports National Bureau of Standards research and development in physics, mathematics, chemistry, and engineering. Comprehensive scientific papers give complete details of the work, including laboratory data, experimental procedures, and theoretical and mathematical analyses. Illustrated with photographs, drawings, and charts.

Published in three sections, available separately:

• Physics and Chemistry

Papers of interest primarily to scientists working in these fields. This section covers a broad range of physical and chemical research, with major emphasis on standards of physical measurement, fundamental constants, and properties of matter. Issued six times a year. Annual subscription: Domestic, \$9.50; \$2.25 additional for foreign mailing.

• Mathematical Sciences

Studies and compilations designed mainly for the mathematician and theoretical physicist. Topics in mathematical statistics, theory of experiment design, numerical analysis, theoretical physics and chemistry, logical design and programming of computers and computer systems. Short numerical tables. Issued quarterly. Annual subscription: Domestic, \$5.00; \$1.25 additional for foreign mailing.

• Engineering and Instrumentation

Reporting results of interest chiefly to the engineer and the applied scientist. This section includes many of the new developments in instrumentation resulting from the Bureau's work in physical measurement, data processing, and development of test methods. It will also cover some of the work in acoustics, applied mechanics, building research, and cryogenic engineering. Issued quarterly. Annual subscription: Domestic, \$5.00; \$1.25 additional for foreign mailing.

TECHNICAL NEWS BULLETIN

The best single source of information concerning the Bureau's research, developmental, cooperative, and publication activities, this monthly publication is designed for the industry-oriented individual whose daily work involves intimate contact with science and technology—for *engineers, chemists, physicists, research managers, product-development managers, and company executives*. Annual subscription: Domestic, \$3.00; \$1.00 additional for foreign mailing.

NONPERIODICALS

Applied Mathematics Series. Mathematical tables, manuals, and studies.

Building Science Series. Research results, test methods, and performance criteria of building materials, components, systems, and structures.

Handbooks. Recommended codes of engineering and industrial practice (including safety codes) developed in cooperation with interested industries, professional organizations, and regulatory bodies.

Special Publications. Proceedings of NBS conferences, bibliographies, annual reports, wall charts, pamphlets, etc.

Monographs. Major contributions to the technical literature on various subjects related to the Bureau's scientific and technical activities.

National Standard Reference Data Series. NSRDS provides quantitative data on the physical and chemical properties of materials, compiled from the world's literature and critically evaluated.

Product Standards. Provide requirements for sizes, types, quality, and methods for testing various industrial products. These standards are developed cooperatively with interested Government and industry groups and provide the basis for common understanding of product characteristics for both buyers and sellers. Their use is voluntary.

Technical Notes. This series consists of communications and reports (covering both other agency and NBS-sponsored work) of limited or transitory interest.

Federal Information Processing Standards Publications. This series is the official publication within the Federal Government for information on standards adopted and promulgated under the Public Law 89-306, and Bureau of the Budget Circular A-86 entitled, Standardization of Data Elements and Codes in Data Systems.

Consumer Information Series. Practical information, based on NBS research and experience, covering areas of interest to the consumer. Easily understandable language and illustrations provide useful background knowledge for shopping in today's technological marketplace.

NBS Special Publication 305, Supplement 1, Publications of the NBS, 1968-1969. When ordering, include Catalog No. C13.10:305. Price \$4.50; \$1.25 additional for foreign mailing.

Order NBS publications from:

Superintendent of Documents
Government Printing Office
Washington, D.C. 20402

U.S. DEPARTMENT OF COMMERCE
National Bureau of Standards
Washington, O.C. 20234

OFFICIAL BUSINESS

Penalty for Private Use, \$300

POSTAGE AND FEES PAID
U.S. DEPARTMENT OF COMMERCE

